

AD-771 913

AD 771 913

USADACS Technical Library



5 0712 01010168 0

TECHNICAL LIBRARY

COPY NO. _____

TECHNICAL REPORT 4590

SHOCK-SHOCK INTERACTION STUDIES FOR WEAK INCIDENT SHOCKS



H. E. HUDGINS, JR.
AND
E. M. FRIEDMAN

DECEMBER 1973

APPROVED FOR PUBLIC RELEASE; DISTRIBUTION UNLIMITED.

AMCMS CODE 5911.21.20676

19970924 132

DTIC QUALITY INSPECTED

PICATINNY ARSENAL
DOVER, NEW JERSEY

The findings in this report are not to be construed
as an official Department of the Army position.

DISPOSITION

Destroy this report when no longer needed. Do not
return to the originator.

Technical Report 4590

SHOCK-SHOCK INTERACTION STUDIES
FOR WEAK INCIDENT SHOCKS

by

H. E. Hudgins, Jr.
and
E. M. Friedman

DECEMBER 1973

Approved for public release; distribution unlimited.

AMCMS Code 5911.21.20676

Engineering Sciences Division
Feltman Research Laboratory
Picatinny Arsenal
Dover, New Jersey

TABLE OF CONTENTS

	Page No.
ABSTRACT	1
CONCLUSIONS & RECOMMENDATIONS	2
INTRODUCTION	4
DISCUSSION	6
One-Dimensional Methods	6
Two-Dimensional Methods	11
Mach Reflection	14
RESULTS	18
REFERENCES	24
APPENDIX A	27
PRIMUS Input Description	27
PRIMUS Key Output Quantities	28
Listing of PRIMUS	30
Check Cases for PRIMUS	54
FIGURES	58
1. Step-Wise Representation of Density Variation Across Shock Layer	58
2. Basic Geometry and Nomenclature of 2-D Analysis	59
3. McDonnell-Douglas Prediction of Mach Reflection Bounds for DNA Sled Test	60

4. Comparison of Cone and Equivalent Wedge Solutions for Oblique Regular Reflection	61
5. Comparison of Wedge Shock-Shock Methods for Oblique Intercept	62
6. DNA Sled Test 4B-B3 - Comparison of Several Theories and Experiments	63
7. Ratio of the Peak Pressure Behind the Reflected Shock Wave to the Initial Cone Pressure vs the Shock-Shock Wave Mach Number- <u>PRIMUS</u> and Experiment, 9° Cone Models	64
8. Ratio of the Peak Pressure Behind the Reflected Shock Wave to the Initial Cone Pressure vs the Shock Wave Mach Number- <u>PRIMUS</u> and Experiment, 15° Cone Models.	65
9. Ratio of the Peak Pressure Behind the Reflected Shock Wave to the Initial Cone Pressure vs Model Mach Number- <u>PRIMUS</u> , NOL, and Experiment, 9° Cone Models	66
10. Ratio of the Peak Pressure Behind the Reflected Shock Wave to the Initial Cone Pressure vs Model Mach Number- <u>PRIMUS</u> , NOL, and Experiment, 15° Cone Models.	67
11. Ratio of the Peak Pressure Behind the Reflected Shock Wave to the Initial Cone Pressure vs the Shock Wave Mach Number- Theory and Experiment, 9° Cone Models.	68
12. Ratio of the Peak Pressure Behind the Reflected Shock Wave to the Initial Cone Pressure vs the Shock Wave Mach Number- Theory and Experiment, 15° Cone Models.	69

13. PRIMUS Predictions for DNA Sled Test Geometry and Blast Strength at Flight Mach Numbers of 3, 5, and 7 as a Function of Intercept Angle	70
14. Comparison of Maximum Shock-Shock In- duced Surface Pressure with Side-on Pressure	71
15. Comparison of Two Weak Blast Cases for Validity of Hypersonic Similitude	72
DISTRIBUTION LIST	73

ABSTRACT

The shock-shock interaction problem for weak incident waves impinging on a supersonic cone has been examined. The purpose of this study was to establish methods for predicting surface pressures since existing methods have been found inadequate for practical problems with weak blast waves. It is shown in this study that one-dimensional theory, which works well for strong blast waves, fails when the components normal to the surface of the flight velocity and of the blast particle velocity become comparable. As a consequence, an axisymmetric two-dimensional solution method was developed using a "primary wave" approximation. This approach has been automated in the PRIMUS computer code. The predictions from the code have been checked against experiment and other theory. The comparisons are presented and the agreement is quite good. The code was also used to predict the cone pressures for DNA Sled Test experiments. The results are presented and compared with the experimental results and other theoretical predictions.

This study established that for weak blast waves the maximum pressure for regular reflection occurs at the Mach reflection limit, not at side-on intercept. The question of whether reflection pressures are even higher on the Mach reflection side of the boundary was examined, but existing prediction methods could not resolve this point. To answer this question, a two-dimensional finite-difference code was also developed for shock-interaction. The feasibility of the method was established, but sufficient calculations have not been conducted at this time to report. It is clear that this finite-difference code could resolve the question definitively upon full development.

CONCLUSIONS

1. The results from "primary wave" analytical approaches developed for both one and two-dimensional problems compare well with exact methods and with experiment within the regular reflection regime.
2. One-dimensional methods have proven insufficient for side-on intercept of conical bodies by weak incident waves at supersonic vehicle velocities.
3. The two-dimensional analytical method has been proven by comparison with experiment to give good estimates of reflection pressures on cones in the regular reflection regime. This method has been automated as the PRIMUS (PRImary Interaction Method for Understanding Shocks) computer program.
4. Regular reflection computations indicate a rapid rise in pressure as the Mach reflection limit is approached, reaching pressures that are about 10% higher than in the side-on situation. These few computations suggest that hypersonic similarity parameter correlation of pressure is still valid for side-on intercept in the weak blast case but that the correlation loses accuracy near the regular reflection pressure maximum which occurs at the regular-Mach reflection boundary.
5. Previously available analytical and numerical estimates of oblique Mach reflection are contradictory and insufficient to settle the question: is there a maximum in shock-shock induced pressure in the Mach reflection regime just before the transition to regular reflection.
6. A two-dimensional finite-difference method using the frozen cells technique has been demonstrated to be feasible. Additional effort and computer time is needed however to produce useful computations in both the Mach and regular reflection regimes to settle the above question.

RECOMMENDATIONS

It is recommended that:

1. the PRIMUS computer program, that was developed, be used for making shock-shock estimates for cones and wedges in the regular reflection regime,
2. an effort should be made to complete the two-dimensional finite-difference method since this seems to be the only computational method capable of settling, once and for all, the question of the magnitude of oblique Mach reflection pressures, .
3. should the completed two-dimensional finite-difference code demonstrate that the Mach reflection regime pressure peak is not the maximum, it should be used to check the PRIMUS code in the regular reflection regime,
4. if this check of the PRIMUS code indicates that it needs to be refined for a more exact calculation of the complete pressure-time history, an effort to make these refinements should be undertaken since PRIMUS requires 1/1000 (or less) of the computer time required by the finite-difference method in the regular reflection regime,
5. improvement of these prediction methods be made before or, at worst, in parallel with further experimental efforts in the shock-shock area.

INTRODUCTION

Shock-shock interaction is the phrase used to refer to the events initiated when the bow wave of a supersonic vehicle encounters an incident wave from an external source, such as a blast wave. It has been known since the early 1960's that such an interaction may result in a transient pressure rise on the vehicle just inside the incident wave front.

The concern of vehicle designers about the effect of this rapid loading and unloading was originally directed toward basic structural integrity. Thus, the mid-60's saw a number of development efforts intended to produce analytical and/or experimental evaluation of shock-shock loading for strong blast waves and hypersonic vehicle velocities. Picatinny Arsenal was actively involved under both DASA, DNA, and AMC sponsorship and produced analytical studies and computer codes in the shock-shock problem area, (Refs 1 to 5).

In order to meet designer's needs, the SLAN computer code was also developed at Picatinny (Ref 6). This code is not an analytical method but utilizes curve fits to the analytical results developed at Picatinny and elsewhere. Its purpose was to estimate shock-shock interaction loading at a blunt body stagnation point and for oblique regular and Mach reflection on cones while requiring a minimum of input and using a minimum of computer time.

In order to cover the wide range of intercept angles and vehicle geometries cited above, a great many assumptions had to be made and hypotheses accepted without adequate verification. This was clearly stated and experimental confirmation called for in the SLAN report. The development of a facility capable of obtaining the required experimental data had been initiated at Picatinny Arsenal. The feasibility study had been completed and a pilot facility was being tested for performance, (Ref 7), when all work on shock-shock interaction was stopped because there did not appear to be any structural damage problem.

Shock-shock interaction loading reappeared as a problem in a different area of vehicle damage in 1972. This time, the concern was with weak incident waves and lower flight Mach numbers. These conditions invalidated many of the assumptions of the SLAN code - warning messages to this effect are printed as part of its output. They also placed analytically based numerical approaches such as the PASS code (Ref 2) in regimes where the numerics did not converge. Some outside user's still persisted in using the SLAN code and in disseminating the results without including the warnings issued by the code itself (for an example, see Ref 8). This resulted in a decision to see what one and two-dimensional analyses could be quickly performed in order to produce valid answers in the weak wave regime now of interest. The results of this effort are presented in this report.

DISCUSSION

One-Dimensional Methods

The numerical difficulties encountered by the PASS code for weak incident shocks required that a different analytical/numerical approach for incident shock with less than a 4 to 1 pressure ratio be utilized. At the same time, it appeared desirable to use as much already available technology as possible.

Picatinny Arsenal had available a transonic unsteady finite-difference axisymmetric flow field computer program (Ref 9). Part of this code consisted of a subroutine to compute which types of wave forms will evolve from the juxtaposition of two states of a gas. Its analytical basis is taken directly from the analysis beginning on page 362 of Landau and Lifshitz (Ref 10) except that it has been specialized to the same gas on both sides. Other subroutines taken from the transonic program are used to iterate to the solution which matches the analytical jump conditions (Rankine-Hugoniot equations) across both waves and meets the required equality of pressure and velocity across the contact surface separating them.

The analytical simplifications made for the computation of shock-shock interaction in the weak wave case were that:

1. the gas is ideal,
2. the continuously varying vehicle flow field properties between the bow shock and the surface are replaced by a number of discontinuous steps with the properties evaluated as the average of the end point values of each strip across the shock layer; the exceptions being that the correct values are used at the shock and at the surface (see Fig 1),

3. when computing the interaction at each node only the primary wave transmitted toward the body is followed from node to node, secondary interactions and waves are ignored.

The heart of the method used lies in the second and third simplifications above. This means that the method used is essentially the method of Moeckel (Ref 11) extended to unsteady flow and it is also related to "shock-expansion" methods. The method developed will henceforth be referred to as the 'primary wave' method. The bounds on validity imposed by the kinds of simplifications made in the primary wave method can only be determined by comparison with exact solutions or with experiments. The resulting new one-dimensional computer code using this method was given the acronym WISH (Weak Interaction of SHocks).

At the same time, a one-dimensional "shock-tube" unsteady finite-difference code using the linear method of Godunov (Ref 12) was modified to compute the one-dimensional shock interaction with the desired pre-interaction flow field. The usual difficulty with this approach is that the desired flow field does not remain constant in time because it does not satisfy the one-dimensional flow equations. It was found that this change occurred more rapidly than the shock-shock interaction and wall reflection did for the cases of interest. Thus, valid answers required a method of preserving the desired flow field for a sufficiently long time period. The technique developed here was a cell-by-cell "freezing" of the desired flow field imposed near the wall end of the "shock-tube." The criterion used for unfreezing a particular cell was a 1% change in the pressure of the adjacent up-stream cell due to shock-shock interaction.

Both of the above methods were checked by comparing with other computations, an experiment, and with each other. The comparison cases used were:

1. NOL experiment: flight Mach number (M_∞) of 5.16, blast Mach number (M_b) of 4.89, head-on intercept of a sphere, (Ref 4);

2. PASS code result: side-on intercept of a 5° cone, $M_\infty = 10.0$, blast pressure ratio (P_b / P_∞) = 21, ideal air;

3. Analytical: shock of pressure ratio 1.5 propagating into still air and reflecting normally from a fixed wall.

These cases were all computed with the WISH code and with the one-dimensional finite-difference code, which was given the name 1-D. A comparison of results is given below:

Table 1

One-Dimensional Comparison

CASE NO.	1st REFLECTION PRESSURE (psf)				TIME TO 1st WALL REFLECTION (microseconds)		
	Exp/Theo	PASS	WISH	1-D	PASS	WISH	1-D
1	3,300 (Exp)	3,280	3,300	3,300	54.4	55.3	57.
2	--	42,360	41,940	41,800	9.88	10.0	10.
3	4,733 (Theo)	--	4,730	4,730	--	74.6	75.

All results are seen to be in good agreement with each other for both pressure and time. It would also appear that any limitations due to the neglect of secondary wave interactions and real gas effects in WISH do not manifest themselves for nearly equal

strength shocks, each with a pressure ratio of about 30 to 1, (Case 1) nor for two very different shock strengths of pressure ratios 21 and 5 (Case 2).

The next step was to see if one-dimensional methods could produce usable results for the side-on intercept of cones with weak blast waves and significant non-parallelism of body and body shock. The case selected for analysis was based on the DNA Shock-Shock Test Program utilizing a rocket sled (Ref 8). An 11.2° cone at Mach 5 was intercepted by a blast wave of pressure ratio 1.6 parallel to the bow shock of the cone (16.6° from the horizontal). The reflected pressures predicted are compared below and can be seen to be in good agreement with each other.

Table 2
Sled Test Pressure Comparison

CODE	1st REFLECTED PRESSURE
WISH	148 psia
1-D	143 psia

The questioning of the validity of a one-dimensional analysis in the weak blast conical case basically arises from one point. Any one-dimensional analysis assumes (among other things) that the incident wave, bow shock, and body surface are parallel. The calculations above made the incident shock and the bow shock parallel and let the cone surface become non-parallel. Next the WISH code was used to compute the case where the incident shock and the cone surface were parallel but the bow shock was not. The result was a wall reflection pressure of 95 pounds per square inch. This large difference indicates that one-dimensional analysis is not adequate.

The question then becomes why was a one-dimensional analysis adequate for stronger incident waves (pressure ratios of 5 to 201) and thin vehicle shock layers (Ref4)? The answer seems to lie in the relative values of the blast particle velocity and the component of cone flight velocity normal to the blast front and, hence, in momentum and energy. When, for example, Check Case #2 and the Sled Test input conditions to the WISH code are compared, the numbers are those given below.

Table 3
SIDE-ON INPUT CONDITIONS COMPARISONS

CASE	CHECK CASE #2	DNA SLED TEST
Vehicle Mach No.	10.0	5.0
Blast Pressure Ratio	21.0	1.6
Blast Particle Velocity	3274 fps	388 fps
Cone Half-Angle	5.0°	11.2°
Cone Shock Angle	7.7°	16.6°
Flight Velocity ⊥ Bow Shock	1296 fps	1588 fps
Flight Velocity ⊥ Cone Surface	843 fps	1080 fps

It is clear that the major difference between the cases is that in the strong wave case the blast particle velocity is 70 to 80% of the sum of normal vehicle

velocity and blast particle velocity, while in the weak wave case the proportions are just about reversed and the vehicle velocity component dominates. In the latter situation the choice of whether the blast wave is parallel to the body surface or parallel to the body shock has a substantial effect upon the resulting total velocity in body-fixed coordinates. Conversely, in the strong incident shock case, the total velocity is relatively insensitive to whether the blast is aligned with the body surface or with the body shock since so much of the total velocity is due to the blast particle velocity. It is also clear that the thicker the shock layer, the greater the difference between the component of the flight velocity normal to the body surface and the component normal to the body shock.

As a result the use of one-dimensional analyses for the weak wave case, which is dominated by a two-dimensional flow, is not appropriate.

Two-Dimensional Methods (Planar and Axisymmetric)

It is well established from experiment (Ref 13 to 15) that the initial interaction between a conical shock and an incident wave can be treated as a planar two-dimensional problem. This interaction can be solved exactly by the SWIVEL code available at Picatinny Arsenal. The SWIVEL code is also capable of computing the regular reflection pressure and duration of the transient due to the transmitted incident wave when the wave propagates through a constant property layer after the shock-shock interaction, i.e., the case of a wedge, (See Fig 2 for the basic wave diagram and designation of regions).

The non-uniform shock layer of a cone was treated by the same basic method of using a step-wise approximation of a non-uniform shock layer with which the transmitted incident wave interacts and ignoring the secondary interactions. The SWIVEL code's analytical basis is the computation of the 4-shock intersection that can result when 2 co-planar waves interact. Thus in the new analysis, the isentropic compression between shock and surface

on a cone was modeled by a series of weak shock compressions since, as is well known, weak shocks are very nearly isentropic.

During the development of the new computer code, it was found that a single interior shock compression to the cone surface conditions gave essentially the same reflection pressure as a multi-shock compression. It was also found that for the cone flight conditions of interest, that the entropy jump across a single interior shock was still small enough that the flow was nearly isentropic. Therefore, in the interest of simplicity of coding, getting results sooner, and ease of setting up cases a single shock compression was used. The new computer code was given the acronym PRIMUS (PRImary Interaction Method of Understanding Shocks). PRIMUS also retains the wedge case capability of the SWIVEL code.

Another change that had to be made in SWIVEL to produce PRIMUS was the addition of the ability to compute the quasi-steady conditions on a cone at an angle of attack. The wedge conditions can be, and still are, computed in closed form but the cone conditions at angle of attack can not. Windward ray cone surface pressures at angle of attack are estimated from experimental data collected and correlated by one of the authors in the form of the ratio of actual pressure coefficient to the Newtonian pressure coefficient vs the hypersonic similarity parameter defined by $M_\infty \sin(\theta_c + \alpha)$, where M_∞ is the flight Mach number, θ_c is the cone semi-angle, and α is the angle of attack. Other properties required were taken from Sims' tabulation for cones at small angles of attack (Ref 16) and curve fitted. The curve fits are restricted to the range of parameters currently expected to be required and they have not been checked for accuracy at flight Mach numbers less than 3, or cone half-angles greater than 15° . Furthermore, Sims' angle of attack data is only valid at small angles of attack.

The original SWIVEL code estimated the duration of the pressure transient by assuming that: the reflected

wave was not deflected or altered in strength by its interaction with the contact surface, the expansion wave resulting from the interaction of the reflected wave and the deflected bow wave also propagated back to the body through uniform conditions, and that this expansion was the primary pressure relief mechanism. The duration was defined so that the decay time due to the width of the expansion fan was excluded. This analysis has not been altered at this time in PRIMUS. Thus, the times predicted for the conical case have been computed using the same basic assumptions. Of course the uniform conditions used are the true cone surface conditions. A desirable future effort would be to incorporate the complete non-uniform layer including interaction with the contact surface.

In parallel with this development, an effort was made to modify a two-dimensional, unsteady finite-difference blunt body flow field program (Ref 17), developed with DNA funding, to compute shock-shock interaction of a plane shock wave with a conical flow field. This approach allows the realistic approximation of two-dimensional effects by allowing for non-parallel body surface, bow shock and blast wave and for the non-uniform shock layer, which is the main flow difference between wedges and cones. This is modeled by the "freezing" of the imposed conical flow just as has been discussed for the one-dimensional finite difference code.

This approach is the only one to date which offers hope for answering certain questions that have been asked in the technical community as to where the maximum wall pressure occurs as a function of intercept angle: is there a maximum on the Mach reflection side of the transition intercept angle from Mach to regular reflection and is it greater than the rise in pressure on the regular reflection side of the transition. The finite difference method is expected to compute both with equal facility. Its one serious drawback would seem to be long running times (about one hour on a CDC 6500 which would make it a candidate for answering certain questions about phenomenology rather than a code to be used for each case of

interest. The "frozen flow field" used in the one-dimensional finite-difference code and now incorporated into the two-dimensional code does not affect the propagation rate of discontinuities nor reflected pressures. All the unsteady finite-difference methods of lower dimensionality than the real problem do share one difficulty: they compute the final quasi-steady-state solution of the lower-dimensionality problem rather than that of the problem they are being used to approximate. This is not an insuperable problem and it can be resolved by the same non-numerical method used in the PASS code; one estimates the width of the final expansion wave and its strength by simple closed form methods (page 78 of Ref 18) and patches this onto the finite difference solution beginning at the first predicted pressure relief at the body surface.

This study was carried to the point of showing feasibility. The code was modified to planar two-dimensional form, the boundary conditions suitably modified and initial conditions for the shock-shock interaction problem coded and debugged. A true wedge case for regular reflection was set up (as the correct result was known) and the computation begun. The initial interaction of the bow and blast waves proceeded normally and the transmitted blast wave was propagated toward the body surface; then the body surface pressure near the nose began to rise as it should. Unfortunately, at this time development work had to cease. The method appears to be verified as to feasibility and a small effort would determine its accuracy for wedge regular reflection, cone side-on at high Mach number, and Mach reflection for cones or wedges, both head-on and oblique.

Mach Reflection

The question has arisen, provoked by some predictions of Gardner (Ref 20) and two experimental points in Ref 19, as to where the maximum shock-shock interaction surface pressure as a function of intercept angle actually occurs. Gardner at McDonnell-Douglas suggests that it lies at the boundary between Mach and regular reflection on the Mach

reflection side and may exceed any regular reflection pressure. To illustrate this, the results from Ref 20 has been redrawn as Fig 3 of this report.

The experimental pressure ratios in Ref 19 are for a 90° half-angle cone at Mach 3.1 and a blast pressure ratio of 5. The PRIMUS code predicts the result for HARTS Round 7 (40° intercept angle) to within the indicated uncertainty and predicts the limit for regular reflection to be between 39.5° and 39.0° . It is HARTS Round 9, which was supposedly at a 41° angle of intercept, which gave an 80% higher value of reflected pressure. Since the angle of attack of the cone and angle of intercept of the blast are both subject to some uncertainty, this may be evidence for a maximum in pressure just on the Mach reflection side of the limit if the combined effect was to reduce the effective angle of intercept below about 39° . On the other hand, it may be evidence for an error in data acquisition or reduction.

A brief survey of existing analytical work that applies to oblique Mach reflection reveals very little of direct applicability to the cases of interest. Blankenship and Busemann (Ref 21) present some calculations for cones with very small intercept angles (1° or less away from head-on). These results apply to a wave pattern which occurs only at very high vehicle Mach numbers ($M_\infty \gg 10$) for the blast strengths of interest. These calculations can only give an initial slope, which certainly does not remain constant, for the variation with intercept angle while the intercept angles of interest are 20 to 30 degrees. Most fundamentally, the assumed wave pattern does not apply to the flight and blast Mach numbers of current interest.

The wedge analysis and results by Inger (Ref 22) appears, at first glance, to be applicable. His assumption of a weak blast wave is consistent with the current problem and the same method is used for intercept angles from 0° (head-on) to 60° . The assumption of a wedge need

not disqualify this method for useful cone computations, (see the comparison in Fig 4). However, Inger's method also requires a strong bow wave and he appears unwilling to extend his method below a value of the hypersonic similarity parameter of about 2 (see Fig 7 of Ref 22). Upon closer examination, one finds that the restrictions are even more severe. Not only must the hypersonic similarity parameter be large but this must be achieved while keeping the wedge and wedge shock essentially parallel. This implies small wedge angles and high Mach numbers. Thus the range of proposed validity seems to be at too high Mach numbers and for too slender wedges to be of use in the current problem area. Nevertheless, one might hope to at least answer the important question of the trend of peak pressure with intercept angle as it increases from head-on. Inger's method shows a smooth steady increase in peak pressure with increasing obliquity of intercept.

The stated range of validity is that the original wedge shock angle (θ) minus the wedge angle (δ), (all in radians, see also Fig 2) is much less than 1. However, the results seem erroneous, at least for large intercept angles, even in this proposed range of validity. The PRIMUS code computes the exact solutions for shock-shock interactions on wedges which result in regular reflection from the surface. A check case of a 6° wedge at Mach 20 (for which the angular difference is 0.04 radians) with a blast wave of Mach number 1.2 was computed with PRIMUS for intercept angles from 60° to 22° . Results for this case were also computed using the correlations plots in Ref 22. A comparison of reflection pressure/ambient pressure is shown below and plotted in Fig 5.

Table 4

Oblique Intercept Comparison for Wedges

INTERCEPT ANGLE (0° = head-on)	$\left(\frac{P_{refl}}{P_\infty}\right)$ Inger	$\left(\frac{P_{refl}}{P_\infty}\right)$ PRIMUS (Exact)
10°	12.60	Mach Reflection
20°	13.10	Mach Reflection
25°	13.38	16.11
30°	13.68	15.89
40°	14.41	16.01
50°	15.45	16.24
60°	17.11	16.45

Since the same pre-intercept and quasi-steady pressures were used for both methods for each case, it seems that the difference must be attributed to the value of maximum pressure computed by Inger's method. That method does not predict the minimum in pressure followed by a strong rise with decreasing intercept angle just before the Mach reflection limit that is characteristic of weak incident wave regular reflection. Either Inger's method cannot be applied to as large intercept angles as he believed in 1966 or 0.04 is not $\ll 1$ for his method at $M_\infty = 20$. Since the small perturbation theory used is only valid in the limit as $\delta \rightarrow 0$, this could be the case. Whether or not it is adequate for small intercept angles (Mach reflection) is not well established at this time.

A rather risky extrapolation of cone experimental results in Ref 23 to lower blast strengths and assuming that the hypersonic similarity parameter is a correlating quantity indicates that Inger's results for head-on intercept in this case are in good agreement (see Fig 5). If this is a valid check, and if Inger predicts the correct trend, it indicates that there is no reflection pressure maximum due to Mach reflection. Any rise in pressure near the Mach-regular reflection limit would then be due to the rise which occurs in the regular regime. However, there are too many unconfirmed assumptions to consider the matter settled.

The work of Smyrl (Ref 24) is similar to that of Inger and is applicable to lower flight Mach numbers but it is a linearized analysis which requires that the wedge angle (or wedge angle plus the intercept angle) be small enough that linearization is valid at the desired Mach number. Thus, this method can only give the initial slope of the pressure-intercept angle function for wedges that are intercepted obliquely.

RESULTS

The one-dimensional "primary wave" (WISH code) and finite-difference methods developed (1-D code) were found to be in good agreement with each other and with a number of other exact and experimental results for one-dimensional flow. One-dimensional computations of the DNA Sled Test conditions at a Mach number of 5, an 11.2° half-angle cone with a 16.6° bow wave angle, and a blast pressure ratio of 1.6 indicated that there was a 55% increase in reflected surface pressure in going from a blast wave parallel to the cone surface to a blast wave parallel to the bow shock. Reasons for this difference are detailed in the Discussion and the essential result is that the one-dimensional approximation breaks down at some difference in angle when the three surfaces (blast wave, bow wave, and body) are not parallel. The breakdown occurs at small angles when the vehicle velocity normal to the blast wave dominates the blast particle velocity in the sum of the two terms.

The two-dimensional "primary wave" analytical approximation was automated in a form appropriate for cones in the PRIMUS computer program. Suitable experimental or independent analytical methods to check against are harder to obtain for the oblique intercept of cones. The most suitable predictions available were those by Gardner and Lenertz (MDAC and MMC, respectively, on Fig 2-15 of Ref 8) for the DNA Sled Test. The PRIMUS results are in good agreement with Gardner for pressure and in fair agreement for duration in this case with the blast front nearly parallel to the cone surface. This is shown in Figure 6. Lenertz does not predict durations and the pressure predicted is lower than the other methods. The peak pressure predicted by PRIMUS is 73 to 79 psia, depending on the experimental uncertainty in blast strength and orientation.

The experimental results for the Sled Test are reported in Reference 8. The data in which the most confidence is placed is from the test designated 4B-B3. However, the fact that the high temperature pressure gauges used had too slow a response time and the regular gauges were subjected to a high temperature environment had necessitated a great deal of processing of the raw data. The basic technique was to calibrate the gauges with a shock-tube and use convolution techniques to predict the actual pressures sensed during the rise time of the slower response gauges. Figure 2-15 of Ref 8 shows both the preliminary estimate band and the final estimate of the shock-shock reflection pressure after processing the raw data. The final estimate results in a peak reflected pressure of about 100 psia. This is 32% above the mean estimates of any of the two-dimensional theories including PRIMUS. The final reduced data from the experiment, as taken from Ref 8, are compared with the theoretical predictions on Fig 6. It should be noted however that the gauge in question read the theoretical pre-interaction surface pressure (33 psia) exactly while it read 23% high for the quasi-steady post-interaction pressure. This suggests that the gauge had changed calibration during the shock-shock transient. The PRIMUS predictions and an analytical approximation

from Reference 14 are compared next with a different experiment (Ref 14) which did not depend upon pressure gauges. Since good agreement was achieved with this other experiment, and several theories are in essential agreement for the DNA Sled Test, it would seem that the gauge response problem is the major cause of the disagreement between theory and experiment in that test. Certainly, the experiment was not as definitive as one would have liked. It is understood that a Phase II experiment will be conducted in which it is hoped to eliminate some of the problems mentioned.

The only oblique regular reflection on cones experimental results are those of Ref 14 where pressures are predicted from photographs of shock patterns observed on cone models launched through an oblique shock at 40° from the normal to the cone axis. The incident shock strengths tested are higher than those of interest to the current problem but the cone angles and cone Mach numbers are in the desired range.

The PRIMUS predictions and these experimental results for the ratio of reflected pressure to initial cone pressure are compared in Figures 7 to 10. Only the mean value of the experimental shock wave Mach numbers actually achieved was used at each nominal experimental value for the incident wave strength in the PRIMUS computations. Quite good agreement was found for the variation of the ratio of reflected to initial pressure with shock wave Mach number for both 9° and 15° half-angle cones (see Fig 7 and 8). The PRIMUS predictions of the variation with cone Mach number shows a somewhat stronger dependence on cone Mach number than the experimental data indicates for both 9° and 15° cones, at the higher blast strengths. As the blast strength is reduced, the agreement with experiment becomes better and better and is excellent at the lowest strength tested and should be excellent at the even lower strengths of interest, (see also Fig 9 and 10).

The Two-dimensional theory used in Ref 14 computes the 2-shock interaction exactly but ignores the effect of the non-uniform shock layer on the strength and orientation of the transmitted shock and then computes the reflection at the surface using actual cone surface conditions. The 'primary wave' approach in PRIMUS does consider the non-uniformity of the shock layer. The improvement made by accounting for the change in transmitted wave strength and inclination is discussed below. The predictions of the theory of Ref 14 are always higher than the PRIMUS code predictions. The PRIMUS predictions are clearly in better agreement with experiment for the 90° cones (Fig 9); while in the case of the 150° cones, the data scatter is too great to permit a choice between the two theories (Fig 10). The pressure trends with shock wave Mach number of the two methods can be seen by comparing Fig 7 with 11 and Fig 8 with Fig 12. Again the method used in PRIMUS compares more favorably with experiment for the 90° cones and also appears superior for the 150° cones.

The PRIMUS code achieved this agreement even though various messages-warning of the violation of assumptions-were printed out for some of the required cases. However, these were related to the small angles of attack limit inherent in using Sims' results (Ref 16) for the quasi-steady state or to the duration calculation, which is known to be an approximation. It is hoped that this will not lead to the wholesale neglect of such messages by users as it did with the SLAN code.

The two-dimensional finite difference computer code using a method of "freezing" the imposed preinteraction flow field was brought to the point of proving feasibility of the basic method in two dimensions. The necessity of stopping work prevented checking it against exact solutions for wedges and comparing it with the PRIMUS results for cones. This computer code is the only one which currently has the potential of computing the oblique Mach reflection case and, hence, resolving the uncertainties in this regime dealt with in detail in the Discussion.

In order to permit the ready computation of oblique intercept of cones and wedges in the regular reflection regime, Appendix A of this report contains a brief user's guide to input and output of the PRIMUS code, a listing of PRIMUS, and a wedge and a cone check case.

The PRIMUS code has been used to compute shock-shock results for a cone of semi-angle 11.2° and a blast Mach number of 1.234 at intercept angles from 90° down to the Mach reflection boundary for flight Mach numbers of 3, 5, and 7. The variation of the maximum in surface pressure over ambient pressure with intercept angle and flight Mach number is shown in Fig 13. The maximum reflected pressure ratio at each Mach number is plotted versus flight Mach number on Fig 14. The pressure ratio at an intercept angle of 78.8° (blast wave parallel to cone surface) is also plotted against Mach number on the same figure. This shows that the maximum pressure in the regular reflection regime always occurred at the boundary between Mach and regular reflection, not at the "side-on" conditions, for weak blast waves. At the same blast strength and cone semi-angle, the regular reflection boundary moves to lower intercept angles (more nearly head-on) as the flight Mach number increases. This is due to the stronger bow wave resulting in greater weakening of the transmitted wave. At the same time, however, the reflected pressure over ambient pressure ratio rises with Mach number since the surface pressure rises more strongly with flight Mach number.

The rapid rise in reflection pressure with small changes in intercept angle near the Mach-regular reflection boundary can result in significant errors if the computational angular increment is too large in this region. For example in the above computations at $M_\infty = 5$, if calculations are made at one degree intervals, a ratio of reflection pressure to ambient of 6.02 at $\beta = 25^\circ$ and Mach reflection at 24° is obtained. But when increments of 0.1° are used the pressure ratio becomes 6.36 at 24.2° , with Mach reflection at 24.1° .

When increments of 0.01° are used, the maximum pressure ratio increases still further to 6.44 at 24.18° with Mach reflection at 24.17° (see also Fig 15).

Earlier side-on results for strong blast waves had correlated well with the hypersonic similarity parameter, (Ref 4). In order to see if this remained true for weak blasts, the Sled Test case and a case at twice the Mach number but the same value of the hypersonic similarity parameter were computed with PRIMUS. The results are compared on Fig 15 for the same blast strength at various intercept angles. The side-on ratios of reflection pressure to ambient are nearly equal, however, the Mach 10 results first undershoot then overshoot the Mach 5 results as the intercept angle decreases. The maximum error, at the same angle, occurs near the Mach reflection limits and is about 10%.

REFERENCES

1. Moran, J. P. and Ritter, A., "A Critical Survey of Shock-on-Shock Interaction Theory," TAR-TR-6507 for Picatinny Arsenal, Oct 1965.
2. Taylor, T. D., "Shock-Shock Interaction Theory Including Real Gas and Three-Dimensional Effects," PATR 3319, Apr 1966.
3. Taylor, T. D. and Hudgins, H. E., "Interaction of a Blast Wave with a Blunt Body Traveling at Supersonic Speeds," AIAA JNL, Feb 1968.
4. Hudgins, H. E., "A Correlation of Pressure, Duration, and Impulse Due to the Shock Interaction Transient on Supersonic Vehicles," PATR-3474, Feb 1967.
5. Hudgins, H. E., "Predictions of Shock Interaction Loading by Empirical Formulas Fitted to Exact Numerical Solutions," PATR 3563, Aug 1967.
6. Hudgins, H. E., "SLAN, A Computer Program for Estimating Shock Interaction Loading," PATR 3715, May 1968
7. Taub, P. A., "Development of the Elements of an Oblique Blast Interaction Facility," PATR 3715, May 1968.
8. Patrick, R.E., "Phase I - Defense Nuclear Agency Shock-on-Shock Experiment," Teledyne Brown Engineering SEC-73-SD-0 706, Jul 1973.
9. Masson, B. S. and Friedman, E. M., "Axisymmetric Transonic Flow Calculations," PATR 4271, Oct 1972.
10. Landau, L. D. and Lifshitz, E. M., Fluid Mechanics, Pergamon Press, NY, NY, 1966.
11. Moeckel, W. E., "Interaction of Oblique Shock Waves With Regions of Variable Pressure, Entropy, and Energy," NACA TN 2725, June 1952.

12. Masson, B. S. Massar, G., McCarthy, T., "A Comparison of 1-D Unsteady Flow Field Methods," PATR 3574, Feb 1970.
13. Merrit, D. L. and Aronson, P.M., "Experimental Studies of Shock-Shock Interactions on a 9° Cone, Naval Ordnance Lab., NOLTR 67-182, 26 Jan 1968.
14. Merritt, D. L. and Aronson, P. M. "Oblique Shock Interaction Experiments," Naval Ord Lab., NOLTR 69-108, 29 May 1969.
15. Nicholson, J. E. "Supersonic Vehicle Entry into and Exit from a Blast Wave," Mithras Inc. MC-65-142-R4, Feb 1967.
16. Sims, J. L. "Tables for Supersonic Flow Around Right Circular Cones at Small Angles of Attack," NASA SP-3007, 1964.
17. Masson, B. S. "Two-Dimensional Flow Field Calculations by the Godunov Method," PATR 3575, Jul 1967.
18. Liepmann, H. W. and Roshko, A., Elements of Gas-Dynamics John Wiley & Sons, NY, NY, 1957.
19. Donselman, R. W. and Johnson, R. R., "Hardening Technology Studies, Ballistic Range Test Data and Analysis Report," Lockheed Missile and Space Co. Y-75-65-9 (also BSD TR-66-96), Sep 1965.
20. Gardner, C., "Presentation at McDonnell-Douglas Corp.," Huntington Beach, CA, 13 June 1973.
21. Blankenship, V. D. and Busemann, A., "Shock-Shock Interaction Inside the Mach Reflection Region for Slender Supersonic Bodies", Aerospace Corp. TDR-669 (S6815-70), Nov 1965.
22. Inger, G. R., "The Effect of Blast Wave Incidence Angle on Hypersonic Shock-On-Shock Interaction," Aerospace Corp., TR-669 (6240-20)-8, 25 Mar 1965.

23. Baltakis, F. P., "Shock Interaction Surface Pressures for Hemispherical and Conical Bodies", Naval Ordnance Lab. NOLTR 71-27, 16 Feb 1971.
24. Smyrl, J. L., "The Impact of a Shock-Wave on a Thin Two-Dimensional Aerofoil Moving at Supersonic Speed," J. Fluid Mech. Vol 15, pg 223, 1963.
25. Ruetnik, J. R., "Presentation at McDonnell-Douglas Corp., "Huntington Beach, CA, 13 June 1973.

APPENDIX A

PRIMUS INPUT DESCRIPTION

COLUMN	NAME	FORMAT	EXPLANATION
1-10	M1	F	Flight Mach number
11-20	XIB	F	Blast pressure/ambient pressure ¹
21-30	BETA	F	Blast intercept angle (0° = head-on)
31-40	DELTA	F	Wedge case = wedge angle; deg. Need not be specified if XIL is specified. Cone case = flow deflection angle at conical shock, deg. need not be specified if XIS is specified.
41-50	XIL	F	Pressure ratio across wedge shock. Need not be specified if DELTA is specified for wedge. Surface pressure ratio for cone case.
51-60	CONE	F	Cone half-angle, deg. Blank for wedge case
61-70	XIS	F	Cone shock pressure ratio. Need not be specified if DELTA, conical flow deflec- tion angle, is specified. Blank for wedge case.

¹Analysis currently scaled to ambient pressure = 1, am-
bient sound speed = 1, ambient density = ratio of specific
heats = 1.4.

PRIMUS KEY OUTPUT QUANTITIES¹

MSUBL	flight Mach number
XISUBB	blast pressure/ambient pressure
BETA	incident wave intercept angle (0° = head-on) deg.
GAMMA	ratio of specific heats (constant)
DELTA	wedge angle, or flow deflection angle at conical shock, deg.
ASUBL	ambient sound speed (scaled to 1)
PSUBL	ambient pressure (scaled to 1)
MSUBB	blast wave Mach number
LAMBDA	final state angle of attack, deg.
THETAF	final state <u>wedge</u> shock angle, deg.
XISUBWF	final state <u>wedge</u> pressure/blast pressure
PSUB3F	final state <u>wedge</u> pressure/ambient pressure
P6/P3F	final state <u>wedge</u> reflection pressure/ambient pressure
PSUBF	cone or <u>wedge</u> reflection pressure/ambient pressure
MSUBF	final state <u>cone</u> surface Mach number
THETAC	final state <u>cone</u> shock angle, windward ray, deg.
ALPHAC	final state <u>cone</u> angle of attack, deg.
CONANGL	<u>cone</u> half angle, deg.

PC/P1 cone initial surface pressure/ambient pressure

P6/PC cone reflection pressure/initial cone surface pressure

TAU cone or wedge dimensionless duration of reflection pressure, $t a_1 / b$, where t is the actual time and b is the axial distance from the wedge or cone tip to the point of interest.¹

1) See also Fig 2 for designation of regions and points.

LISTING OF PRIMUS

JUMP 3
 25000 1 1100 FORMAT(1H0,30HSTEADY CONDITIONS FOR POINT A-+/-) SWIVEL 40
 1110 FORMAT(1H,5X,5HVSUH,7X,5HVSUH,7X,5HVSUH,2,7X,5HVSUH,3,5X, - SWIVEL 41
 . 46MEPSA(0EG) SIGMA1(0EG) SIGMA2(0EG) SIGMA3(0EG)) SWIVEL 42
 1120 FORMAT(1H,5X,5HVSUH,7X,5HVSUH,7X,5HVSUH,2,7X,5HVSUH,3,5X, - SWIVEL 43
 . 44MEPSH(0EG) TAU1(0EG) TAU2(0EG) TAU3(0EG)) SWIVEL 44
 1130 FORMAT(1H0,44HCONDITIONS IN REGIONS 4 AND 5- NO SOLUTION) SWIVEL 45
 C 19HPROGRAM TERMINATED) SWIVEL 46
 1140 FORMAT(1H0,30HCONDITIONS IN REGIONS 4 AND 5-+/-) SWIVEL 47
 1150 FORMAT(1H,25H THETA1(0EG) THETA2(0EG)*4X,6HXISUB1,6X,6HXISUB2, - SWIVEL 48
 . 48M SIGMA4(0EG) SIGMA5(0EG) PHI1(0EG) PHI2(0EG),5X, - SWIVEL 49
 . 7METASUH,6X,5M4/A3) SWIVEL 50
 1160 FORMAT(1H,25H THETA1(0EG) THETA2(0EG)*4X,6HXISUB1,6X,6HXISUB2, - SWIVEL 51
 . 48H TAU1(0EG) TAU2(0EG) PS1(0EG) PS2(0EG),5X, - SWIVEL 52
 70 1170 FORMAT(1H0,42HCORDITIONS OF REGULAR REFLECTION. REGULAR) SWIVEL 53
 C 46HREFLECTION LIMIT EXCEEDED. PROGRAM TERMINATE-+/-) SWIVEL 54
 1180 FORMAT(1H0,33HCONDITIONS OF REGULAR REFLECTION-+/-, - SWIVEL 55
 . 48M OMEGAI(0EG) DELTAH(0EG) VSUB4P HSUB4P, - SWIVEL 56
 . 46M THETARP(0EG) UMEGAM(0EG) XISUBR PSUB6,8X, - SWIVEL 57
 . 18MP6/P3 P6/P3F) - SWIVEL 58
 1190 FORMAT(1H0,47HNONOMINAL TIME OF PEAK OVERPRESSURE NOT COMPUTED-) SWIVEL 59
 1200 FORMAT(1H0,34HNONOMINAL TIME OF PEAK OVERPRESSURE-+/-,7X,4HAP/R,8X, - SWIVEL 60
 . 4HCP/R,8X,4HOC/R,8X,4HEP/R,8X,4HOP/R) - SWIVEL 61
 . 1210 FORMAT(1H0,3X,44HCHI(0EG) PS17(0EG) MU7(0EG) - PS1M(0EG)) SWIVEL 62
 . 1220 FORMAT(1H0,3X,5HVSUH,7X,5HVSUH,7X,5HVSUH,7X,5HVSUH,9X,3HTAU) SWIVEL 63
 . 1230 FORMAT(1H0,34HNONOMINAL TIME OF PEAK OVERPRESSURE-+/-,7X,4HAP/R,8X, - SWIVEL 64
 . 4HCP/R,8X,4HOC/R) - SWIVEL 65
 . 1240 FORMAT(1H0,5X,5HVSUH,7X,5HVSUH,7X,5HVSUH,7X,5HVSUH,7X,3HTAU) SWIVEL 66
 1250 FORMAT(1H,34X,51TIME HAS FAILED. TIMEA USED TO EXTRAPOLATE IN 1 SWIVEL 67
 CAU.) - SWIVEL 68
 1260 FORMAT(1H0,10X,22HESTIMATED RESULTS AHE:3X,6HIAU => G12,5,3X,7H6 SPACE 1
 1270 FORMAT(1H0,20X,22HTHIS CASE IS BEING COMPUTED FOR A CONE.) DOPRINT 1
 IP3 = '012,5,0,1 CONE 1
 90 1280 FORMAT(1H,45X,3AHTHIS CASE IS BEING COMPUTED FOR A CONE.) CONE 2
 1290 FORMAT(1H,56X,16HCUNE RESULTS AHE:) CONE 2
 1300 FORMAT(1H,8X,5HMSUH,7X,6HTHE1AC,7X,7HALPHAF,6X,7HCONANGL,7X,5HPC REALP2 2
 1C/PI,8X,5HPC/P,7X,7H PSUB6,5X,6H*SCALE,7X,7HMSCALE,7X,3HTAU,/*4 REALP2 2
 2X,10,1F10,6,3X,0) 3
 95 1400 FORMAT(1H,35X,54HSINGLE STEP SHOCK COMPRESSION TO CONE SURFACE PHS JUMP 4
 1410 FORMAT(1H,28X,12HPCONE/PSHOCK,5X,6HMSUB1,3X,12HSHOCK ANGLE,2X,12H JUMP 5
 1420 FORMAT(1H,28X,12HENHOPY JUMP,2X,12HRLAST ANGLE,28X,7(G12,5,2X JUMP 6
 21,) 1420 FORMAT(1H0,2X,46HTIMES MAY BE IN ERROR - COMPUTATION CONTINUES.) CUNE3 6
 100 10 CONTINUE C DOPRINT 3
 . M=0 INITIAL 1
 . DOPRINT 4
 105 G=1,4 CONEFIX 1
 . GINV=1,1/G TAUB-I 1
 . GP=6,1. SWIVEL 73
 . GM=6,1. SWIVEL 74
 . CON=3,1415927/190. SWIVEL 75
 . CON=3,1415927/190. SWIVEL 76
 . CON=3,1415927/190. SWIVEL 77


```

60 PRINT-1080
60 10 10
70 IF (W .EQ. 1) GO TO 71
PRINT 1090
PRINT 1030,THETA,XIW,ETAW,A3,AM3
PRINT 1100
PRINT 1110
GO TO 100
IF (W .EQ. 1) GO TO 81
80 IF (W .EQ. 1) GO TO 81
81 CALL POINTA(1CASE)
GO TO 100
IF (W .EQ. 1) GO TO 81
82 PRINT 1120
PRINT 1030,V1,V2,V3,EP5,ANG1,ANG2,ANG3
83 CALL FURFIV(NERR)
IF (NERR)120.120.110
110 PRINT 1130
GO TO 10
120 CONTINUE
120 IF (W .EQ. 1) GO TO 122
PRINT 1140
GO TO 1130,140. 1CASE
130 PRINT 1150
GO TO 150
140 PRINT 1160
150 PRINT 1030,THETA,X11,X10,ANG4,ANG5,ANG7,ANG6,ETAT,A4A3
152 IF (CONE .EQ. 0) GO TO 121
IF (W .EQ. 0) PRINT 1280
154 C COMPUTE 1-STEP COMPRESSION TO CONE SURFACE
155 C
155 ALFA=LAMBDAA
ALSAVE=LAMBDA
SAVEH=M2
OLSAVE=DELTA
DELTA=CONE
XSAVE=XIW
CSAVE=A3/A1
IF (INWALL.EQ. 1) GO TO 25
N#ALL=1
XIW=X11/XSAVE
ETAW=XIW**(-GINV)
A3=SOH((XIW*ETAW)
M1=M1
M1=AM3
THETA=ASIN(SQRT((0.5*GPR*(XIW-1.)/6)*1./M1))
SUMN=(ISIN(THETA)*M1)**2
DELTA=ATAN((2.0*(SUMN-1.))/((M1*M1)*(G+COS(2.0*THETA))*2.)*TAN(THETA))
11)
THETA=THETA/CUN
210 C SAVE COMPRESSION SHOCK ANGLE
211 C
212 C DELTA=DELTA/CUN
213 C
214 C
215 C
220 JUMP 13
JUMP 14
JUMP 15
INTERP 2
CONE 14
NUCONE 15
NUCONE 16
NUCONE 17
JUMP 13
JUMP 14
JUMP 15
CONE 14
NUCONE 15
NUCONE 16
NUCONE 17
JUMP 16
JUMP 17
JUMP 18
JUMP 19
JUMP 20
NUCONE 19
NUCONE 20
NUCONE 21
NUCONE 22
NUCONE 23
NUCONE 24
NUCONE 25
NUCONE 26
NUCONE 27
JUMP 28

```

```

DELSOR=(GP/(12.*0*0))*(XIW-1.)*3 JUMP 29
M1=M3 JUMP 30
XIBS=XIB NUCONE 23
XIB=1 JUMP 31
PSCALE=XSAVE NUCONE 24
ASCALE=CSAVE NUCONE 25
GO TO 1500,510, ICASE JUMP 34
500 BE1A=ANGT JUMP 35
60 TO 520 JUMP 36
510 BE1A=40.-ANGT JUMP 37
520 PRINT 1400 JUMP 38
PRINT 1410,XIW,M1,THETA,DELTA,DELSON,BETA JUMP 39
GO TO 20 JUMP 40
25 AMF=SAVEN JUMP 41
ALFA=ALSAVE JUMP 42
CALL FCONE (CONE,XIBS,M1)
CM=U3F/A3F NUCONE 26
IF (M .EQ. 1) GO TO 330 NEGATE 8
PRINT 1060 NUCONE 9
PRINT 1030,LAMBDA,DELTAF,THETAf,XIWf,ETAF,A3F+P3F+U3F NUCONE 28
PRINT 1030, NUCONE 29
C CONVERTING FINAL CONE VALUES TO COMPRESSION VALUES NUCONE 30
C NUCONE 31
C 330 CONTINUE NUCONE 32
XIWf=XIW/PSCALE NUCONE 33
ETAF=ETAF/(PSCALE*(1./G)) NUCONE 34
A3F=A3F/ASCALE NUCONE 35
P3F=P3F/PSCALE NUCONE 36
U3F=U3F/ASCALE NUCONE 37
ALFA=LAMHDA NUCONE 38
ALFA=1 NUCONE 39
NOPHINT 17
I21 CALL REGFL (ICASE,NERR)
IF (NERR) 170,170,160 SWIVEL 120
160 PRINT 1170 SWIVEL 121
NERR=9 SWIVEL 122
170 IF (M .EQ. 1) GO TO 171 SWIVEL 123
171 PRINT 1180 NOPHINT 18
PRINT 1030,OMEGA1,DELTA1,VAP,M4P,THE1A,OMEGAR,XIR,P6,P6P3,P6P3F
171 GO TO 190,190, ICASE NOPHINT 19
180 CALL TIME(NEWH) HEALP2 4
IF (NERR .EQ. 1) GO TO 6969 JUMP 45
181 IF (CONE .EQ. 0.) GO TO 210 SWIVEL 128
181 IF (M .EQ. 1) GO TO 211 CONE3 14
X1=XIW*PSCALE JUMP 46
P6C=XIW*P6P3 INTERP 7
TSCALE=ASCALE JUMP 47
TAU=TAU*ASCALE JUMP 47
TAUX=TAUX*ASCALE JUMP 47
PRINT 1290 CONE 25
GO TO 10 REALP2 5
190 CALL TIME(NERR) DOPHINT 6
IF (N .EQ. 4 .AND. NERR .GT. 0) GO TO 440 TAUB-1 6
IF (NEWH .LE. 0) GO TO 220 SWIVEL 131
M=1 NOPHINT 21

```

```

PRINT 1250
B1=BETA
IF (CONE .NE. 0.) THENA=THOLD
IF (THETA-DELIA .GT. 5.) GO TO 250
IF (THETA-190.-THETA)*.999
NERR=0
P=P*P3
IF (CONE .EQ. 0.) GO TO 261
ASAVE=AMF
THSAVE=THETAS
ALSAVE=ALFA
OSAVE=DELIA
XISAVE=XIM
XISAVE=EXIT
TSAVE=TSCALE
DELTA=DLSE
CONTINUE
N=2
B2=BETA
GO TO 20
200 PRINT 1190
GO TO 10
210 IF (M .EQ. 1) GO TO 211
PRINT 1200
PRINT 1030,APOR,CPOR,OCOR,EPOR+OPOR
PRINT 1210
PRINT 1030, CHI,PSI7,MU7,PS1M
PRINT 1220
PRINT 1030, VC*U7,V7,VE,TAU
IF (N .EQ. 2) GO TO 290
IF (N .EQ. 3) GO TO 300
IF (N .EQ. 4) GO TO 420
GO TO 10
220 IF (M .EQ. 1) GO TO 221
IF (CONE .NE. 0.) GO TO 222
PRINT 1230
PRINT 1030, APOR,CPOR,OCOR
PRINT 1210
PRINT 1030, CHI,PSI7,MU7,PS1M
PRINT 1240
PRINT 1030, VC*U7,V7,TAU
IF (N .EQ. 4) GO TO 420
GO TO 10
222 CONTINUE
X1=X1W*PSCALE
P6C=X1W*P6P3
TSCALE=ASCALE
TAU=TAU*ASCALE
PRINT 1290
PRINT 1300, CM,THETAF,ALFA,DELIA,X1W,P6P3,P6C,PSCALE,TSCALE,TAU
GO TO 10
IF (THEIA-DELIA .GT. 15.) GO TO 200
WRITE (6,1260)
GO TO 260

```

PROGRAM PRIMUS TRACE

```

290 T2=TAU      TAUB=1 18
      NERR=0      TAUB=1 19
      N=3         TAUB=1 20
      BETA=82.5.  TAUB=1 21
      B3=BETA     TAUB=1 22
      IF (CONE .NE. 0.) THETA=THOLD
      IF (CONE .NE. 0.) DELTA=DLSEV
      GO TO 20      JUMP 54
      300 T3=TAU      JUMP 55
      NERR=0      TAUB=1 13
      N=4         TAUB=1 24
      BETA=90.      JUMP 25
      IF (CONE .NE. 0.) THETA=THOLD
      IF (CONE .NE. 0.) DELTA=DLSEV
      B4=HETIA     TAUB=1 26
      GO TO 20      TAUB=1 27
      345 T4=TAU      JUMP 56
      BETA=B1      JUMP 57
      CALL PARA-(T2*13+T4*82+83*84*61*12+C12+C13)
      TAU=CT1*CT2*BETA*CT3*BETA*BETA
      TAU=ABS(TAU)
      P6P3=PA
      IF (CONE .NE. 0.) GO TO 421
      PRINT 1270,TAU,P6P3
      GO TO 10      TAUB=1 28
      421 AMF=ASAVE    DOPRINT 14
      THFTAS=THSAVE  TAUB=1 30
      ALFA=ALSAVE   TAUB=1 31
      DELTA=DSAVE   TAUB=1 32
      XIW=XISAVE    TAU=1 33
      XIT=XTSAVE    CONE3 15
      A1W=XIW*PSCALE
      P6C=XIW*P6P3
      TSCALE=ASCALE
      TAU=TAU*ASCALE
      TAUX=TAU*ASCALE
      PRINT 1290
      PRINT 1300, CH, THETAF, ALFA, DELTA, XIW, P6P3, P6C, PSCALE, TAU
      GO TO 10      CONE 33
      355 422 AMF=ASAVE    DOPRINT 15
      THFTAS=THSAVE  TAUB=1 35
      CONE FIX 21
      ALFA=ALSAVE   TAUB=1 35
      CONE FIX 22
      DELTA=DSAVE   TAUB=1 35
      XIW=XISAVE    TAUB=1 35
      XIT=XTSAVE    CONE3 15
      A1W=XIW*PSCALE
      P6C=XIW*P6P3
      TSCALE=ASCALE
      TAU=TAU*ASCALE
      TAUX=TAU*ASCALE
      PRINT 1290
      PRINT 1300, CH, THETAF, ALFA, DELTA, XIW, P6P3, P6C, PSCALE, TAU
      GO TO 10      CONE 36
      370 440 BETA=B3-2.
      IF (CONE .NE. 0.) THETA=THOLD
      IF (CONE .NE. 0.) DELTA=DLSEV
      B4=BETA
      NERR=U
      GO TO 20      TAUB=1 37
      320 GO TO 10      TAUB=1 37
      6969 WHILE(6,1420)  CONE3 16
      TAU=ABS(TAU)
      GO TO 181      CONE3 17
      380 END          CONE3 18
      SWIVEL          SWIVEL 151
  
```

SUBROUTINE BLSTWV -- TRACE

```

      SUBROUTINE-BESTWV
      REAL M1,M2,M3
      COMMON/HREG/M3,VBN*ETAB,A2*UB*U2,M2
      COMMON/CONST/G,GP,GM,CON,AL,P1
      COMMON/INPUT/M1,X1B,X1A,DELTA
      B=CON*HE1A
      M8=SQRT((GP*X1B*GM)/(2.0*G))
      VBN=M8
      ETAB=(GM*X1B*GP)/(GP*X1B*GM)
      A2=SQRT(X1B*ETAB)
      U2=VBN*M1*COS(H)
      U2=SQRT((M1*SIN(H))**2+(UB-ETAB*VBN)**2)
      M2=U2/A2
      RETURN
      END
      SWIVEL 152
      SWIVEL 153
      SWIVEL 154
      SWIVEL 155
      SWIVEL 156
      SWIVEL 157
      SWIVEL 158
      SWIVEL 159
      SWIVEL 160
      SWIVEL 161
      SWIVEL 162
      SWIVEL 163
      SWIVEL 164
      SWIVEL 165
      SWIVEL 166

```

SUBROUTINE ROWANG TRACE C0C 6600 FTN V3.0-P304 OPT=1 10/25/73 14:09:27. ---- PAGE - - - - - 1

CCOC 6600 FTN V3.0-P304 OPI=1 10/25/73 14-09-27. ----- PAGE ----- 1

BRAUNLINE-BORANGIM: OEL-TA: THE FLAME

卷之三

```

REAL M
COMMON/CNST/G,GP,GM,CON,A1,PI
C SHOCK ANGLE EQUATION IS OF THE FORM OF A BI-CUBIC
C DEFINE CONSTANTS AND COEFFICIENTS OF BI-CUBIC
C
C 5      S NERH=0
C          00=CUN*OELIA
C          SEN=SIN (0D)
C          CUS=COS (0D)
C          C2=(M**2+2.0*FM**2-G*SEN**2
C          D=(2.0*M**2+1.0)/M**4+(GP**2/4.0*GM/M**2)*SEN**2
C          E=CUS**2/M**4
C          P=C*C/3.0
C          Q=2.0*(C/3.0)**3 -C*0/3.0 *E
C          R=0/(2.0*(SQR((-P/3.0)**3)))
C          RAHS=ADS (H)
C          IF (RAHS .GT. 1.0) GO TO 140
C          OMEGA=ACOS (H)
C          CC=2.0*SQRT (-P/3.0)
C
C 20     C TRIGONOMETRIC SOLUTION TO ROOTS OF CUBIC
C
C 25     C
C          RT1=CC*COS (OMEGA/3.0) -C/3.
C          RT2= CC*COS (OMEGA/3.0+120.*CON ) -C/3.
C          RT3= CC*COS (OMEGA/3.0-120.*CON ) -C/3.
C
C 30     C DETERMINE MIDDLE ROOT - THE PHYSICALLY CORRECT ONE
C          SSMALLEST ROOT RESULTS IN AN ENIMOPY DECREASE
C          LARGEST ROOT IS STRONG SHOCK SOLUTION
C
C 35     C
C          X=AMAX1(RT1,RT2,RT3)
C          Y=AMIN1(RT1,RT2,RT3)
C          IF (RT1 .LT. X .AND. RT1 .GT. Y) GO TO 1
C          IF (RT2 .LT. X .AND. RT2 .GT. Y) GO TO 2
C          IF (RT3 .LT. X .AND. RT3 .GT. Y) GO TO 3
C          NEPR=1
C          RETURN
C
C 40     C
C          3 RT=RT3
C          60 TO 4
C
C 45     C
C          1 RT=RT1
C          60 TO 4
C          2 RT=RT2
C
C 50     C SOLUTION FOR SHOCK ANGLE
C
C          4 THETA=(ASIN (TSHY/(ABS (TTHY)*CON
C          130 IF (THETA=90.0) 150,150,140
C          140 NERH=1
C          150 CONTINUE
C          RETURN
C
C 169    SWIVEL
C 170    SWIVEL
C 171    SWIVEL
C 172    SWIVEL
C 173    SWIVEL
C 174    SWIVEL
C 175    SWIVEL
C 176    SWIVEL
C 177    SWIVEL
C 178    SWIVEL
C 179    SWIVEL
C 180    SWIVEL
C 181    SWIVEL
C 182    SWIVEL
C 183    SWIVEL
C 184    SWIVEL
C 185    SWIVEL
C 186    SWIVEL
C 187    SWIVEL
C 188    SWIVEL
C 189    SWIVEL
C 190    SWIVEL
C 191    SWIVEL
C 192    SWIVEL
C 193    SWIVEL
C 194    SWIVEL
C 195    SWIVEL
C 196    SWIVEL
C 197    SWIVEL
C 198    SWIVEL
C 199    SWIVEL
C 200    SWIVEL
C 201    SWIVEL
C 202    SWIVEL
C 203    SWIVEL
C 204    SWIVEL
C 205    SWIVEL
C 206    SWIVEL
C 207    SWIVEL
C 208    SWIVEL
C 209    SWIVEL
C 210    SWIVEL
C 211    SWIVEL
C 212    SWIVEL
C 213    SWIVEL
C 214    SWIVEL
C 215    SWIVEL
C 216    SWIVEL
C 217    SWIVEL
C 218    SWIVEL
C 219    SWIVEL
C 220    SWIVEL
C 221    SWIVEL

```

SUBROUTINE BOWAVE TRACE ----- CDC 6600 FIN V3.0-P304 OPT=1 10/25/73 14:09:27. ----- PAGE 1

```
REAL M1,M2,M3
COMMON/REG/MB*VBN*ETAB*A2*UB*U2*M2
COMMON/CONST/G*GP*GM*CON*A1*PI
COMMON/INPUT/M1,XB*HE1A,DELTA
COMMON/REG/ THE1A,X1*ETAB*A3*AM3
CALL BOWANG(M1,DELTA,1,THETA,NERK)
IF (NERK) 10,10,20
10 T=CON*THETA
      U=CON*DELTA
      AHNS=(M1*SINT))**2
      X1W=(2.0*G*AMNS-GM)/GP
      AM3=SQR((1.0*5*GM*AMNS)/(G*AMNS-0.5*GM))**2
      ETAW=(GM*X1W*GP)/(GP*X1W*GM)
      AJ=SUM1 (X1W*ETAW)
15   20 CONTINUE
      RETURN
      END
```

SUBROUTINE FINAL TRACE PAGE 1

CDC 6600 F7N V3.0-P304 OPT=1 10/25/73 14.09.27.

```
      SUBROUTINE FINAL (INERR)
      REAL M1,MH,M2,LAMH0A
      COMMON/BREG/MB*VBN*ETAB*A2*UBB*U2*M2
      COMMON/CONST/G*GP*GM*CONA1P1
      COMMON/FREG/LAMR0A*DELTAF*THEIAF*XIWF*ETAWF*A3F*P3F*U3F
      COMMON/INPUT/M1*XI0*HETA*DELTA
      B=CON*HETA
      LAMH0A=BEIA-ATAN (M1*SIN (R)/(UB-ETAB*VBN))/CON
      DELTAF=DELTA*LAMH0A
      CALL BOWANG(M2*DELTAF*THEIAF*NERR)
      IF (INERR) 10*10*20
 10  XIWF=(2.*G*M2*M2*SIN (17)*SIN (11)-GM1)/GP
      15  XIWF=(GM*XIWF*GP)/(GP*XIWF*GM)
      20  CONTINUE
      20  RETURN
      END
      30  A3F=SIN (XIWF*ETIAF)*A2
      P3F=XIWF*XIWF
      40  U3F=SIGN (102*COS (11)*2 + (ETAWF*U2*SIN (11))*2)
      41
```

```

SUBROUTINE FORFIV(TNEHK)
REAL M1,MH,M2
COMMON/APOINT/VA*V1*V2*V3*EPS*ANG1*ANG2*ANG3
COMMON/HREG/MB*VBN*ETAB*A2*UR*U2*M2
COMMON/CNST/G,GP,GM,CON,A1,P1
COMMON/INPUT/M1,X1B,BETA*DELTA
COMMON/DIREG/THETA*XI1*XI0*ANG4*ANG5*ANG6*ETAT*-
CA4A3
COMMON/REG/ THETA*XI1*XI0*ETAW*A3*AM3
P4M=(12.0*G*(V3/A3)*2-GM)/GP)*XI4
P5M=(12.0*G*(V2/A2)*2-GM)/GP)*XI8
P3*XI8
P2*XI18
P2*(P4M-PSM) 10.10.20
10  PM=P5M
      10  PM=P5M
      10  GO TO 30
      20  PM=P4M
      30  IF (P3-P2) 40.40.50
      40  PL=P2
      20  A5L=ANG2
      20  PR=P1/P3
      20  CALL POINT(PR,V3*A3,DSIG,ANG)
      20  A4L=ANG3-DSIG
      20  GO TO 60
      50  PL=P3
      25  A4L=ANG3
      25  PR=P1/P2
      25  CALL POINT(PR,V2*A2,DSIG,ANG)
      30  A5L=ANG2+DSIG
      30  60  CALL INSEC (P2*P3,ANG2*ANG3*PM*PL,A4L,A5L,V2*A2*V3*A3*NERR)
      30  60  IF (NERR) 70.70.80
      30  70  ANG1=ANG3-THETAT
      30  70  ANG3=ANG2+THETAD
      30  70  ETAT=(GM*XI1*GP)/(GP*XI1*GM)
      35  70  A4A3=SQRT (XI1*ETAT)
      35  80  CONTINUE
      35  80  RETURN
      35  END

```

SUBROUTINE INTSEC TRACE PAGE 1
 CDC 6600 F7N V3.0-P304 OPT=1 10/25/73 14.09.27.
 SUBROUTINE INTSEC-(P2,P3,S2,S3,PM,PL,S4L,SSL,V2,A2,V3,A3,NERH)
 COMMON/TDHEG/THETAT,THETAD,XIT,XID,ANG4,ANG5,ANG6,ANG7,ANG8,ETAT,
 CA4A3
 DEL=10.0
 5 DO 10 I=1,50
 DEL=DEL/10.0
 PU=PL*DEL
 PRT=PU/P3
 PRO=PU/P2
 CALL POINT(PRO,V2,A2,DS,THETAD)
 SSL=S2*DS
 CALL POINT(PRT,V3,A3,DS,THETAT)
 S4U=S3*DS
 CALL SLIPT(SSL,PL,SSL,PU,S4L,PL,S4U,PU,SO,PO)
 IF (PO-PU) 10,30,40
 10 CONTINUE
 20 NERH=1
 60 TO 90
 30 XIT=PRT
 XID=PHD
 ANG4=S4U
 ANG5=SSL
 NERR=0
 60 TO 90
 DO 70 I=1,1000
 PL=PU
 PU=PO
 S4L=S4U
 SSL=SSL
 PRT=PU/P3
 PRO=PU/P2
 CALL POINT(PRO,V2,A2,DS,THD)
 SSL=S2*DS
 CALL POINT(PHT,V3,A3,DS,THT)
 S4U=S3*DS
 CALL SLIPT(SSL,PL,SSL,PU,S4L,PL,S4U,PU,SO,PU)
 IF (PU-PU) 50,20,20
 50 IF (PU-PU) 20,30,60
 60 IF (ABS (PU-PU)-0.0001) 80,80,70
 70 CONTINUE
 60 TO 20
 80 XIT=PU/P3
 XID=PO/P2
 CALL POINT(XID,V2,A2,DS,THETAC)
 ANG5=S2*DS
 CALL POINT(XIT,V3,A3,DS,THETAT)
 ANG6=S3*DS
 NERR=0
 70 CONTINUE
 90 RETURN
 END

SUBROUTINE POINT TRACE CDC 6600 F7N V3.0-P304 OPT#1 10/25/73 14-09-27. PAGE 1

```
      SUBROUTINE POINT(X1,V1,DEL,ANG)
COMMON/CONST/G,GP,GM,CON,A1,PI
      AA=2.*G*(V/A)*(V/A)-1.)/GP
      BB=X1-1.
      CC=X1*GM/GP
      PW=(AA-BB)/CC
      PH=ABS(PW)
      1 COANG=SUPT(PW)
      AA=G*(V/A)*(V/A)
      DEL=ATAN(BB*COANG/(AA-BB))/CON
      ANG=ATAN(1./COANG)/CON
      RETURN
      END
```

```
      SWIVEL 346
      SWIVEL 347
      SWIVEL 348
      SWIVEL 349
      SWIVEL 350
      SWIVEL 351
      SWIVEL 352
      SWIVEL 353
      SWIVEL 354
      SWIVEL 355
      SWIVEL 356
      SWIVEL 357
      SWIVEL 358
```

CDC 6600 F7N V3.0-P304 OPT=1 10/25/73 14:09:27. PAGE 1

SUBROUTINE POINTA TRACE

```
      SUBROUTINE POINTA(LCASE)
      REAL M1,M2,M3
      COMMON/APOINT/VA,VI,V2,V3,EPS,ANG1,ANG2,ANG3
      COMMON/BREG/MM,VBN,ETAB,A2,U8,U2,M2
      COMMON/CONST/G,GP,GM,CUN,A1,P1
      COMMON/INPUT/M1,X1B,BETA,DELTA
      COMMON/WREG/THETA,XIW,ETAW,A3,AM3
      B=CUN*HETA
      T=CON*THETA
      ANG=90.-THETA
      IF (THETA-ANG) 10,10,20
 10  ICA>E=1
      VA=UB/COS -(B+T)
      IF (ICA>E) 40,40,15
      15  V1=SQRT ((M1*SIN (T))**2+(VA-M1*COS (T))**2)
          V2=SQRT ((ETAB*VBN)**2+(VA*SIN (B+T)-M1*SIN (B))**2)
          V3=SQRT ((ETAW+M1*SIN (T))**2+(VA-M1*COS (T))**2)
          EPS=ATAN (M1*SIN (T))/(VA-M1*COS (T))/CON
          ANG1=90.-THETA-EPS
          A=CON*(190.-BETA-THETA-EPS)
          ANG2=BETA+ATAN (ETAB*TAN (A))/CON
          E=CON*EPS
          ANG3=90.-THETA-ATAN (ETAW*TAN (E))/CON
          GO TO 30
 20  ICASE=2
      VA=-UB/COS -(B+T)
      IF (ICA>E) 25,25,30
      25  S0  V1=SQRT ((M1*SIN (T))**2+(VA-M1*COS (T))**2)
          V2=SQRT ((ETAB*VBN)**2+(VA*SIN (B+T)-M1*SIN (B))**2)
          V3=SQRT ((ETAW+M1*SIN (T))**2+(VA-M1*COS (T))**2)
          EPS=ATAN (M1*SIN (T))/(VA-M1*COS (T))/CON
          ANG1=THEIA-EPS
          A=CON*(BETA+THETA-EPS-90.)
          ANG2=90.-BETA+ATAN (ETAB*TAN (A))/CON
          E=CON*EPS
          ANG3=THEIA-ATAN (ETAW*TAN (E))/CON
          30  CONTINUE
          RETURN
          END
      35
      40
      45
      50
      55
      60
      65
      70
      75
      80
      85
      90
      95
      100
      105
      110
      115
      120
      125
      130
      135
      140
      145
      150
      155
      160
      165
      170
      175
      180
      185
      190
      195
      200
      205
      210
      215
      220
      225
      230
      235
      240
      245
      250
      255
      260
      265
      270
      275
      280
      285
      290
      295
      300
      305
      310
      315
      320
      325
      330
      335
      340
      345
      350
      355
      360
      361
      362
      363
      364
      365
      366
      367
      368
      369
      370
      371
      372
      373
      374
      375
      376
      377
      378
      379
      380
      381
      382
      383
      384
      385
      386
      387
      388
      389
      390
      391
      392
      393
      394
      395
```

SUBROUTINE REGFL TRACE ----- CDC 6600 F7N V3.0-P304 OPT=1 10/25/73 14.09.27. PAGE - 1

```
      SUBROUTINE REGFL (ICASE, NERR)
      REAL M1, M4P, LAMRDA
      COMMON/APOINT/VA*V1, V2*V3, EPS, ANG1, ANG2, ANG3
      COMMON/CONST/G, GP, GH, CON, A1, P1
      COMMON/FREG/LAMRDA, DELTIAF, THEIAF, XINF, ETAWF, A3F, U3F
      COMMON/INPUT/AN1, A1B, B1A, DELTA
      COMMON/WREG/OMEGA1, DELTAM, V4P, M4P, THETAM, OMEGAR, XIR, P6, P6P3, P6P3F
      COMMON/TDREG/THETAI, THEIAU, XIU, XIU, ANG4, ANG5, ANG6, ETAT, CA4A3
      COMMON/WREG/ THETIA, XIN, ETAW, A3, AM3
      GO TO 110, 20, ICASE
      10  OMEGAI=90.-UELTIA-ANG1
      GO TO 30
      20  OMEGAHS (DELTIA-ANG1)
      30  U=CON*OMEGA1
      I=CON*THEIAF
      DELTAM=OMEGA1-ATAN (ETAT*TAN (U))/CUN
      60  V4P=V3*SIN (T)*SURT (ETAT**2*(1./TAN (0))**2)
      M4P=V4P/(A4A3)
      IF (OMEGA1=.02) .L1. 0.0. GO TO 70
      CALL BOMANG(M4P, DELTAR, THETAR, NERR)
      1F (NERR) 40*40*50
      40  T=CON*THETAR
      OMEGAR=THETAR -DELTAR
      XIR=(2.*G*M4P*M4P*SIN (T)*SIN (T))**GP
      25  CONTINUE
      80  P6=XIN*XIT*XIW
      P6P3=XIN*XIT
      P6P3F=P6/P3F
      30  50  CONTINUE
      RETURN
      70  PRINT 100
      100 FORMAT(1HO *TRANSMITTED BLAST WAVE PARALLEL TO BODY - IGNORE - VE
      1LUCITY AND TIME OUTPUTS*,/)
      35  OMEGA=0.0001
      OMEGAI=0.0001
      THETAM=0.0001
      DELTAM=0.0001
      XIR=(13.*G-1.)*XIT-GM)/(GM*XIT-GP)
      GO TO 60
      40  END
```

SUBROUTINE SLIPI TRACE

CDC 6600 FIN V3.0-P304 OPT=1 10/25/73 14-09-27. PAGE 1

```
SUBROUTINE SLIPI(X1,Y1,X2,Y2,X3,Y3,X4,Y4,A,B,C,D)
A=(Y1-Y2)/(X1-X2)
B=0.5*(Y1+Y2-A*(X1+X2))
C=(Y3-Y4)/(X3-X4)
D=0.5*(Y3+Y4-C*(X3+X4))
X=(D-B)/(A-C)
Y=0.5*(H+U+C*(A+C))
RETURN
END
```

```
SWIVEL 426
SWIVEL 427
SWIVEL 428
SWIVEL 429
SWIVEL 430
SWIVEL 431
SWIVEL 432
SWIVEL 433
SWIVEL 434
```

ROUTINE	TIME	ROUTINE	TIME
SUBROUTINE	TRACE	SUBROUTINE	1
COMMON/M4P/	REAL M1,M4P.	COMMON/AH01N	COMMON/AH01N
COMMON/CONST	COMMON/CONST	COMMON/FREG/	COMMON/FREG/
COMMON/INPUT	COMMON/INPUT	COMMON/HMEG/	COMMON/HMEG/
COMMON/TORG	COMMON/TORG	CA4A3	COMMON/TIME/
	COP0H*TAU		COP0H*REG/
	COMMON/REG/	100	FORMAT(1//0.39
	T=CON*IMETA		T=CON*IMETA
	O=CON*OELTA		O=CON*OELTA
	AI=CON*ANGT		AI=CON*ANGT
	AO=CON*ANGD		AO=CON*ANGD
	O=CON*OMEGA_K		O=CON*OMEGA_K
	OI=CON*OMEGA_A		OI=CON*OMEGA_A
	APOR=51Y (T-		APOR=51Y (T-
	CP0H=AP0H*SI		CP0H=AP0H*SI
	AA=SIN (T)-A		AA=SIN (T)-A
	BB=CUS (T)-A		BB=CUS (T)-A
	CHI=ATAN (AA)		CHI=ATAN (AA)
	C=CON*CHI		C=CON*CHI
	OC0H=30H (A		OC0H=30H (A
	VC=OC0H*VA		VC=OC0H*VA
	U7=U3F		AA=VC*SIN (C
	BB=VC*CUS (C		BB=VC*CUS (C
	PSI7=ATAN (A		PSI7=ATAN (A
	V7=SQRT (AA*		V7=SQRT (AA*
	CNST=A3F/V7		CNST=A3F/V7
	IF (CNST <LE.		IF (CNST <LE.
	CNST=1.		CNST=1.
	WHITE16=IU0)		WHITE16=IU0)
	MU7=ASIN (C		MU7=ASIN (C
	PSIM=PS17*MU		PSIM=PS17*MU
	PH=CON*PSIM		PH=CON*PSIM
	EPOR=CP0H*SI		EPOR=CP0H*SI
	AA=COS (T)-A		AA=COS (T)-A
	OP0H=AA/CUS		OP0H=AA/CUS
	VE=(COPH-EPU		VE=(COPH-EPU
	TAU=EP0H/AA		TAU=EP0H/AA
	IF (TAU <LE.		IF (TAU <LE.
	RETURN		END

--CDC 6600 F1N V3.0-P304 OPT=1 10/25/73 14:09:27, -- PAGE 1
 SWIVEL 435
 SWIVEL 436
 SWIVEL 437
 SWIVEL 438
 SWIVEL 439
 SWIVEL 440
 SWIVEL 441
 SWIVEL 442
 SWIVEL 443
 SWIVEL 444
 SWIVEL 445
 JUMP 73
 SPACE 2
 SWIVEL 448
 SWIVEL 449
 SWIVEL 450
 SWIVEL 451
 SWIVEL 452
 SWIVEL 453
 SWIVEL 454
 SWIVEL 455
 SWIVEL 456
 SWIVEL 457
 SWIVEL 458
 SWIVEL 459
 SWIVEL 460
 SWIVEL 461
 SWIVEL 462
 SWIVEL 463
 SWIVEL 464
 SWIVEL 465
 SWIVEL 466
 SWIVEL 467
 SWIVEL 468
 SWIVEL 469
 SWIVEL 470
 SWIVEL 471
 SWIVEL 472
 SWIVEL 473
 SWIVEL 474
 SWIVEL 475
 SWIVEL 476
 SWIVEL 477
 SWIVEL 478
 SWIVEL 479
 SWIVEL 480
 SWIVEL 481

*ANG2,ANG3
 *INF,ET1WF,A3F,P3F,U3F
 *METAH,OMEGAR,XIR,P6,P6P3,P6P3F
 *ANG4,ANG5,ANG6,ANG7,ANG8,ET1,
 PS17,U7,V7,MU7,PSIM,EPOR,VE,
 (U-0)
 (U-0)

-90-DEGREES.-ERROR PROBABLE.-

10/25/73 44-9-27: PAGE 1

SUBROUTINE WEDGE TRACE ----- COC 6600 F7N V3.0-OP304 OPT=1 10/25/73 14:09:27. ----- PAGE 1
 SUBROUTINE WEDGE(X1,M1,DELTA,THETA) -----
 C THIS CODE COMPUTES THE WEDGE AND SHOCK ANGLE WHEN THE WEDGE
 C SURFACE PRESSURE RATIO AND THE AMBIENT MACH NUMBER ARE SPECIFIED
 C
 5 REAL MS, M1
 C
 C MS=M1
 C THETA=ASIN (SQR ((6.0*X1)+1.0)/(7.0*MS)))
 10 C DELTARATAN(1./TAN(THETA))*S.0*(MS*SIN(THETA))*SIN(THETA)-1.0)/(6.0*H
 C CS= S.0*(MS*SIN (THETA))*SIN (THETA)-1.0))
 C
 C 1 THETA=THETA*57.296
 15 C DELTA=DELTA*57.296
 C RETURN
 C END
 C
 C SWIVEL 531
 C SWIVEL 532
 C SWIVEL 533
 C SWIVEL 534
 C SWIVEL 535
 C SWIVEL 536
 C SWIVEL 537
 C SWIVEL 538
 C SWIVEL 539
 C SWIVEL 540
 C SWIVEL 541
 C SWIVEL 542
 C SWIVEL 543
 C SWIVEL 544
 C SWIVEL 545
 C SWIVEL 546
 C SWIVEL 547
 C SWIVEL 548
 C SWIVEL 549

SUBROUTINE PARA TRACE

CDC 6600 FITN V3.0-P304 OPT=1 10/25/73 - 14:09:27. PAGE 1

```
ROUTINE PARA -(Y1*Y2+Y3*X1,X2,X3,CON1,CON2,CON3)
CON2=((X2*X3*X3)*(Y1-Y2)-(X1*X1-X2*X2)*(Y2-Y3))/_
C ((X2*X2*X3*X3)*(X1-X2)-(X1*X1-X2*X2)*(X2-X3))
CON3=((Y1-Y2)-CON2*(X1-X2))/(X1*X1-X2*X2)
CON1=Y1-CON2*X1*CON3*X1*X1
RETURN
END-
```

5

CDC 6600 FIN V3.0--P304 OPT=1 10/25/73 14.09.27. PAGE -- 2

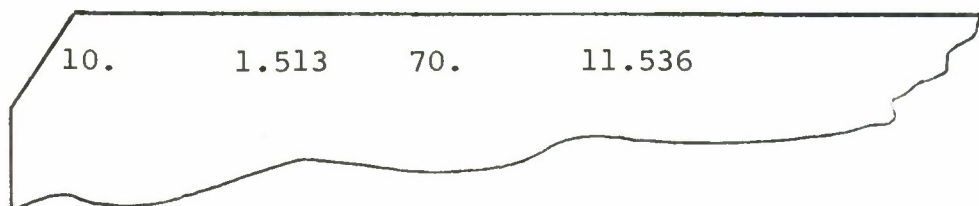
SUBROUTINE FCONE TRACE

CHECK CASES FOR PRIMUS

1. Wedge

Flight Mach Number = 10., Wedge Angle=11.536°
Blast Pressure Ratio = 1.513, Intercept Angle=70°

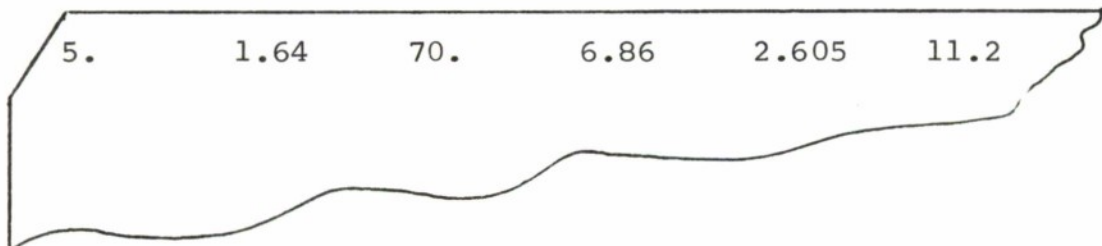
INPUT CARD



2. Cone (flow deflection at shock specified)

Flight Mach Number = 5., Cone Semi-Angle=11.2°
Blast Pressure Ratio = 1.64, Intercept Angle=70°

INPUT CARD



OBlique BLAST WAVE REFLECTION FROM WEDGE ON CONE IN SUPERSONIC FLOW

INPUT CONDITIONS-

MSUB1	XISUBB	BETA(0EG)	DELTA(0EG)
10.00000	1.51300	70.00000	11.53600

CONSTANTS-

GAMMA	ASUB1	PSUB1
1.40000	1.00000	1.00000

CONDITIONS ACROSS BLAST WAVE-

MSUBB	VSUBAN	ETASUBB	ASUB2	USUBB	USUB2	MSUB2
1.19988	1.19988	.74549	1.06204	4.62008	10.10852	9.51807

NEW STEADY STATE CONDITIONS. (F), ATTACHED FINAL BOW SHOCK-

LAMBDA(0EG) DELIAF(0EG) THETA(0EG)	XISUBWF	ETASUBWF	ASUB3F	PSUB3F	USUB3F
1.62679 13.16279 18.05207	9.98260	.26246	1.71906	15.10367	9.64603

CONDITIONS ACROSS BOW WAVE, ATTACHED BOW SHOCK-

THETA(0EG) — XISUBW — ETASUBW	ASUB3	MSUB3
16.07256 8.77565 .27539	1.55458	6.20061

STEADY CONDITIONS FOR POINT A-

VSUBA	VSUBI	VSUB2	VSUB3	EPSA(0EG)	SIGMA1(0EG)	SIGMA2(0EG)	SIGMA3(0EG)
67.45333 57.91043	57.90491	57.90491	57.84924	2.74020	71.16723	70.88512	73.17228

CONDITIONS IN REGIONS 4 AND 5-

THETA(0EG) THETAF(0EG)	XISUBT	XISUBD	SIGMA4(0EG)	SIGMA5(0EG)	PHI1(0EG)	PHI2(0EG)	ETASUBI	A4/A3
1.75300 2.74748	1.34515	7.80210	72.83893	72.83893	71.41929	73.63260	.80975	1.04366

CONDITIONS OF REGULAR REFLECTION-

OMEGA1(0EG) DELIAR(0EG)	VSUB4P	MSUB4P	THETARY(0EG)	OMEGAR(0EG)	XISUBR	PSUBR	P6/P3	P6/P3F
7.04471 1.33037	14.39180	8.87038	7.33142	6.00105	1.32816	15.67939	1.78658	1.03805

NOMINAL TIME OF PEAK OVERPRESSURE-

AP/R	CP/R	OC/R	EP/R	OP/R
.94492	.13253	.22544	.15849	.35682
CHI(0EG)	PSI1(0EG)	MU7(0EG)	PSIM(0EG)	
15.05949	21.12487	17.84243	38.96730	
VSUHC	VSUB7	VSU87	VSU8E	IAU
15.20690	9.64603	5.61051	13.37757	.03389

OBlique BLAST WAVE REFLECTION FROM WEUGE ON CONE IN SUPERSONIC FLOW

INPUT CONDITIONS

MSUB1	XISUBH	BETA(0DEG)	DELTA(0DEG)
5.00000	1.64000	70.00000	6.86000

CONSTANTS

GAMMA	ASUB1	PSUB1
1.40000	1.00000	1.00000

CONDITIONS ACROSS BLAST WAVE

MSUBB	VSUBBN	EISUBB	ASUB2	USUBB	MSUB2
1.24442	1.24442	0.70480	1.07511	2.95452	5.13725

NEW STEADY STATE CONDITIONS. (1) ATTACHED FINAL BOW SHOCK

LAMBDA(0DEG) DELTA(0DEG) THETA(0DEG)	XISUBWF	EISUBWF	ASUB3F	PSUB3F	USUB3F
3.85293 10.71293 20.55649	3.11760	0.46269	1.29125	5.11287	4.88202

CONDITIONS ACROSS BOW WAVE, ATTACHED BOW SHOCK

THETA(0DEG)	XISUBW	EISUBW	ASUB3	MSUB3
16.58992	2.21104	0.57556	1.12809	4.30977

STEADY CONDITIONS FOR POINT A

VSUBA	VSUB1	VSUB2	VSUB3	EPSA(0DEG)	SIGMA1(0DEG)	SIGMA2(0DEG)	SIGMA3(0DEG)
49.67075	44.90159	44.89291	45.88641	1.82197	71.58812	71.11944	72.36120

CONDITIONS IN REGIONS 4 AND 5

THETA(0DEG) THETA(0DEG)	XISUBT	XISUBD	SIGMA4(0DEG)	SIGMAS(0DEG)	PHI1(0DEG)	PHI0(0DEG)	tISUBT	A4/A3
1.74970	1.91164	1.55536	2.09693	71.84115	71.89115	70.61150	73.03108	1.06647

THIS CASE IS BEING COMPUTED FOR A CONE

SINGLE STEP SHOCK COMPRESSION TO CONE SURFACE PRESSURE

Pcone/PSHOCK	MSUB1W	SMUCK-ANGLE	DEFL.-ANGLE	ENTROPY-JUMP	BLAST-ANGLE
1.1782	4.3098	14.425	1.5364	0.5720E-03	70.611

OBlique BLAST WAVE REFLECTION FROM WEUGE ON CONE IN SUPERSONIC FLOW

INPUT CONDITIONS-

MSUB1	X1SUBR	BETA1(0EG)	DELTA1(0EG)
4.3977	1.55536	70.6150	1.53639

CONSTANTS-

GAMMA	ASUB1	PSUB1
1.40000	1.00000	1.00000

CONDITIONS ACROSS BLAST WAVE-

MSUBR	VSUBR	EISUBR	ASUBR	USUBR	USUB2	MSUB2
1.21492	1.21492	0.73125	1.06647	2.64564	4.42889	4.15286

NEW STEADY STATE CONDITIONS. (F). ATTACHED FINAL BOW SHOCK-

LAMBOA(0EG)	DELTAf(0EG)	THETAf(0EG)	X1SUBWF	EISUBWF	ASUBWF	PSUBWF	USUBWF
3.98770	5.52408	17.8335	1.73067	0.7908	1.15615	2.69181	4.31490

CONDITIONS ACROSS R0 WAVE. ATTACHED BOW SHOCK-

THETA1(0EG)	X1SUBW	EISUBW	ASUB3	MSUB3
14.42542	1.17818	0.88959	1.02377	4.18238

STEADY CONDITIONS FOR POINT A-

VSUBA	VSUB1	VSUB2	VSUB3	EPSA(0EG)	SIGMA1(0EG)	SIGMA2(0EG)	PHID(0EG)	ETASUB1	A4/A3
30.58057	26.42869	26.41549	26.42394	2.32826	73.24631	72.53883	73.50313	75.01225	1.06485

CONDITIONS IN REGIONS 4 AND 5-

THETA1(0EG)	THETA1(0EG)	X1SUBT	X1SUBD	SIGMA4(0EG)	SIGMA5(0EG)	PHIT(0EG)	PHID(0EG)	ETASUB1	A4/A3
2.68572	2.47341	1.53980	1.16639	72.7583	72.79583	70.81742	75.01225	73.640	1.06485

THIS CASE IS BEING COMPUTED FOR A CONE

NEW STEADY STATE CONDITIONS. (F). ATTACHED FINAL BOW SHOCK-

LAMBOA(0EG)	DELTAf(0EG)	THETAf(0EG)	X1SUBF	EISUBWF	ASUBWF	PSUBWF	USUBWF
3.85243	11.20000	15.90160	3.52043	0.40957	1.29105	5.77432	5.48085

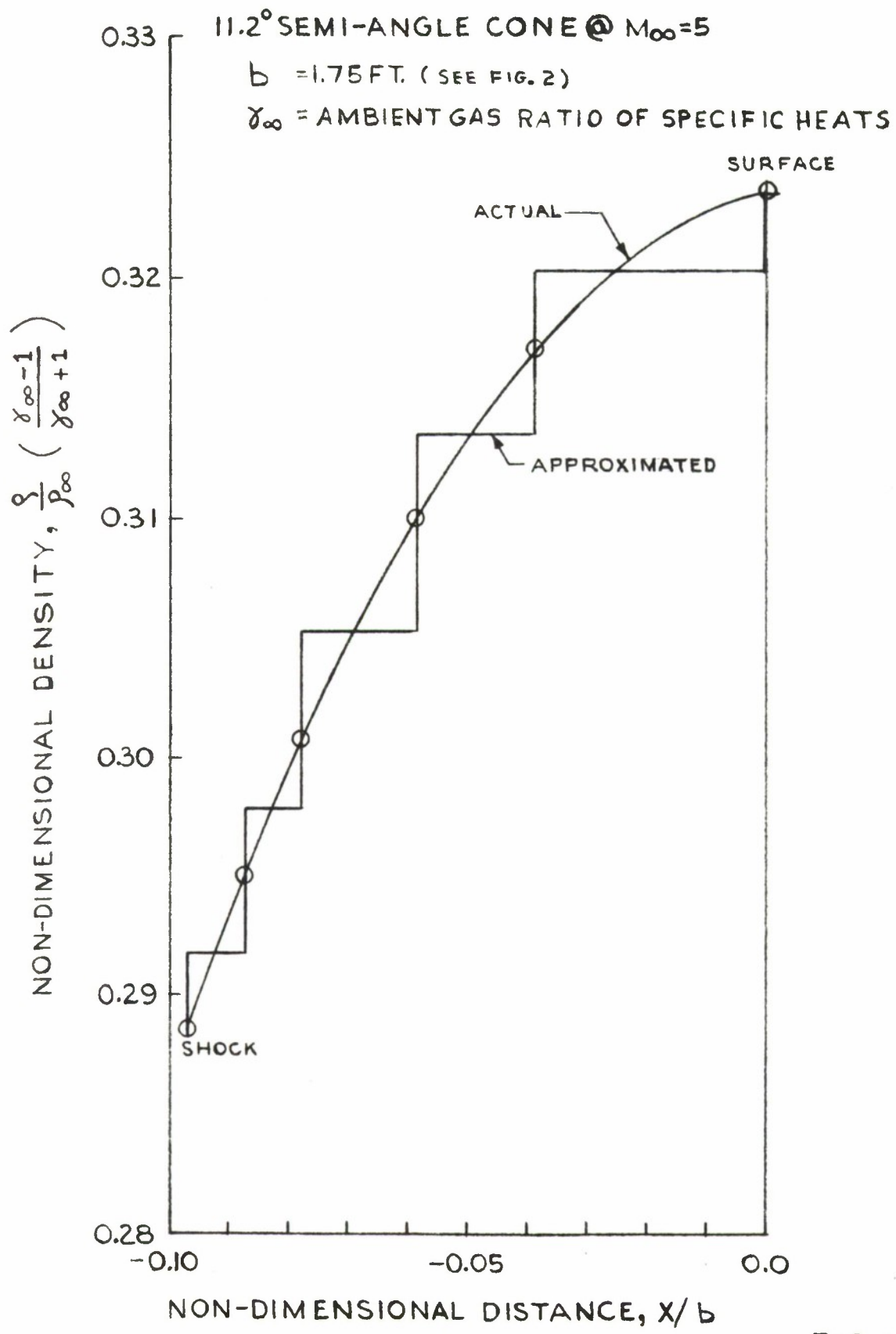
CONDITIONS OF REGULAR REFLECTION-

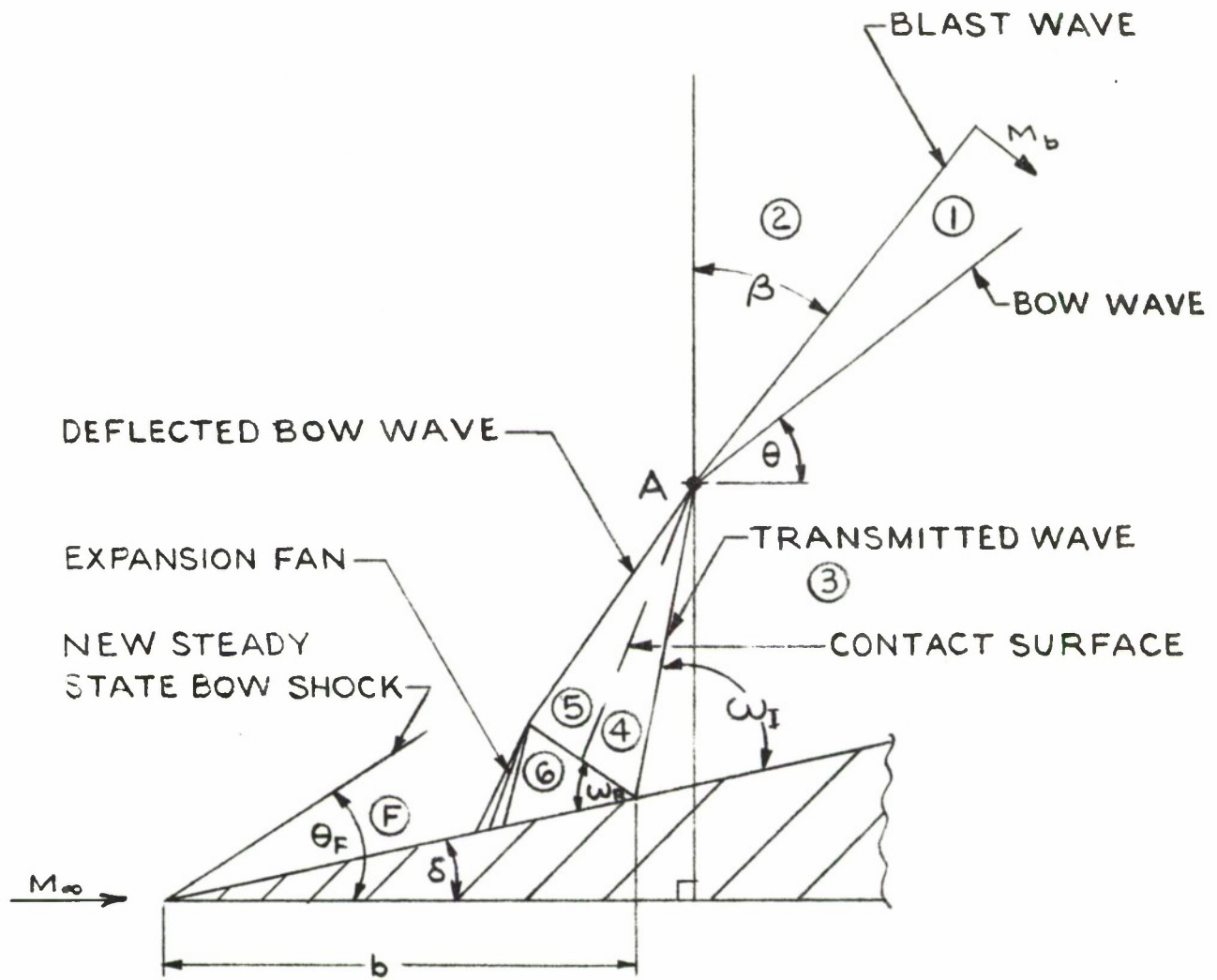
OMEGA1(0EG)	DELTA1(0EG)	VSUB4P	MSUB4P	THETARY(0EG)	OMEGA1(0EG)	X1SUBR	PSUB6	P6/P3	P6/P3F
7.98258	2.06811	8.87637	8.14231	8.49865	6.35184	1.49904	2.71949	2.30822	1.04132

COME RESULTS ARE

MSUBF	THETAC	ALPHAC	CONANG	PC/PI	P6/PC	PSUB6	PSCALE	JASCALE	JAU
4.24525	15.901597	3.852930	11.200000	2.60499	2.308223	6.012918	2.21104	1.128087	0.647

DENSITY VARIATION ACROSS SHOCK LAYER





BASIC GEOMETRY AND NOMENCLATURE OF 2-D ANALYSIS

MCDONNELL-DOUGLAS PREDICTION OF MACH REFLECTION
BOUNDS FOR DNA SLED TEST.

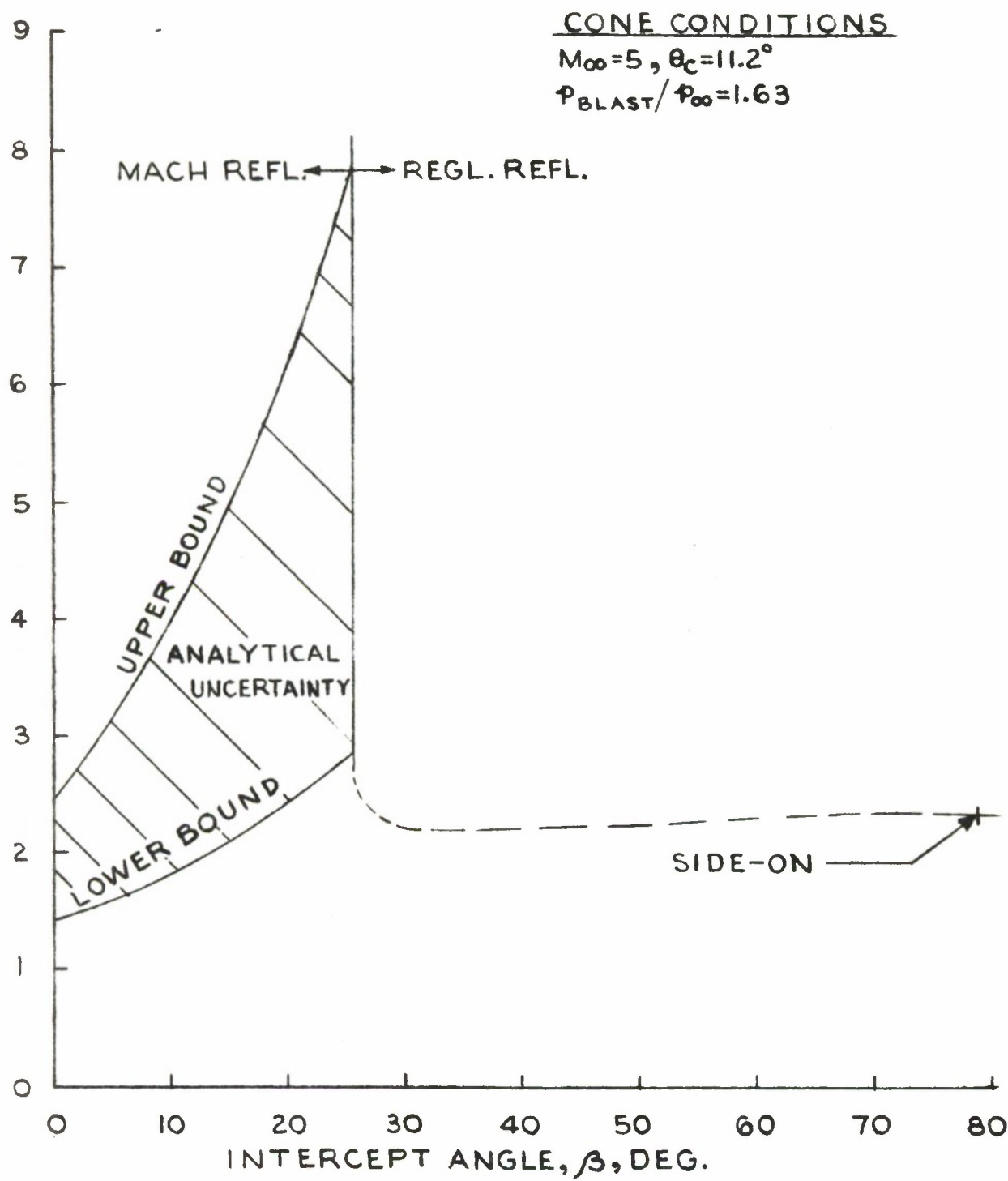


FIG. 3.

COMPARISON OF CONE AND WEDGE SOLUTIONS

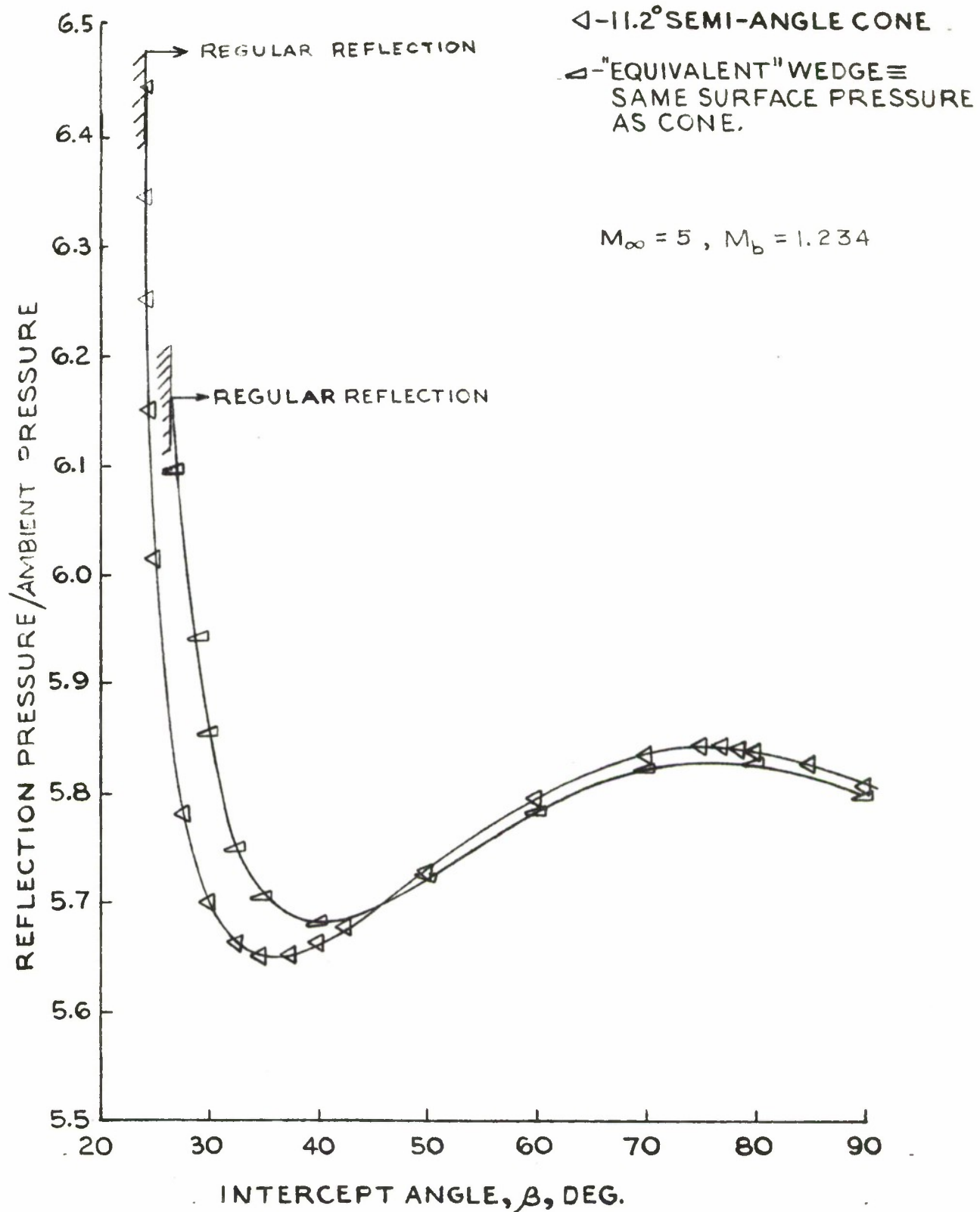
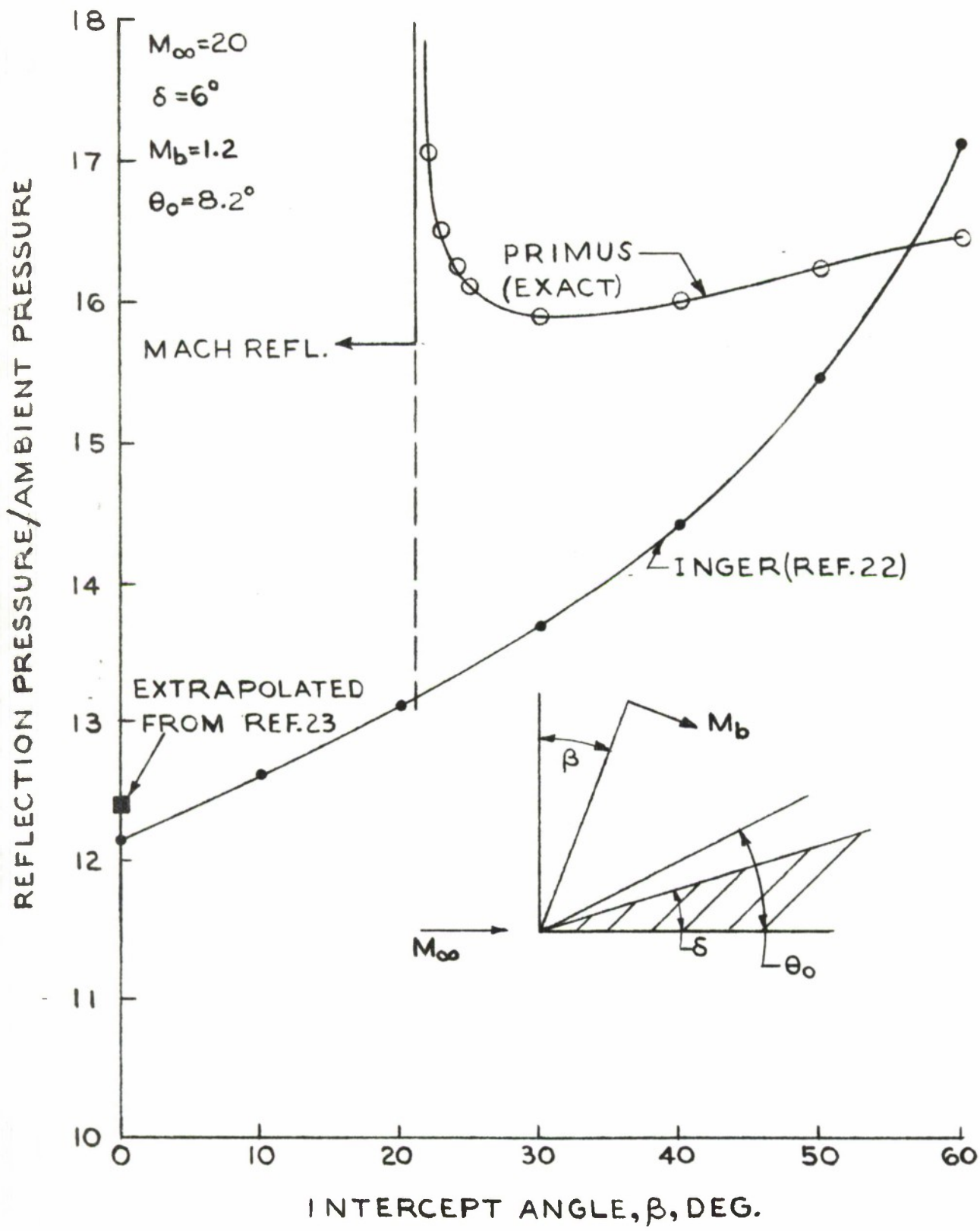


FIG.4.

COMPARISON OF WEDGE SHOCK-SHOCK METHODS



DNA SLED TEST 4B-B3-COMPARISON OF SEVERAL THEORIES AND EXPERIMENT.

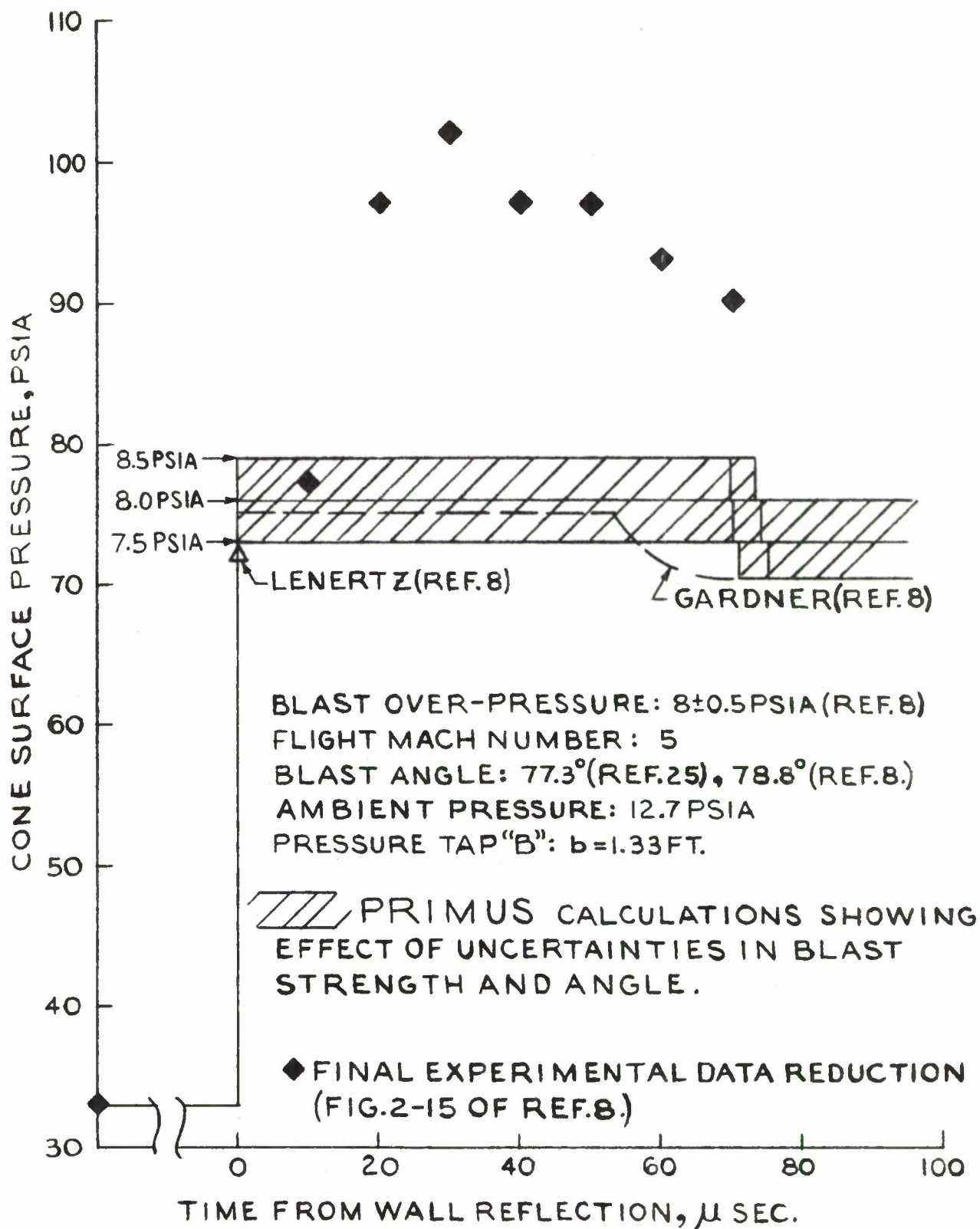


FIG. 6

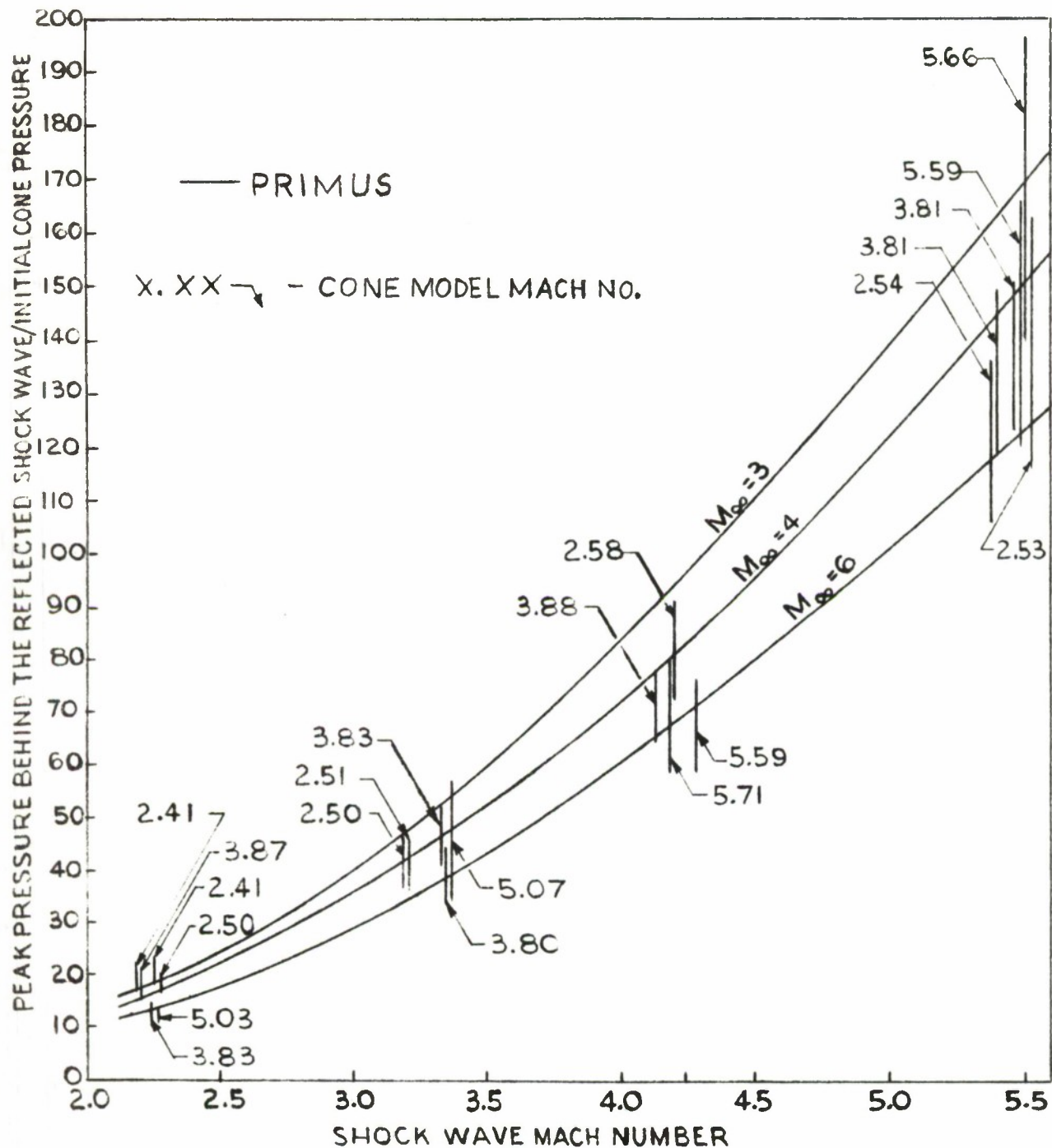


FIG. 7 RATIO OF THE PEAK PRESSURE BEHIND THE REFLECTED SHOCK WAVE TO THE INITIAL CONE PRESSURE VS. THE SHOCK WAVE MACH NUMBER - PRIMUS AND EXPERIMENT, 9° CONE MODELS

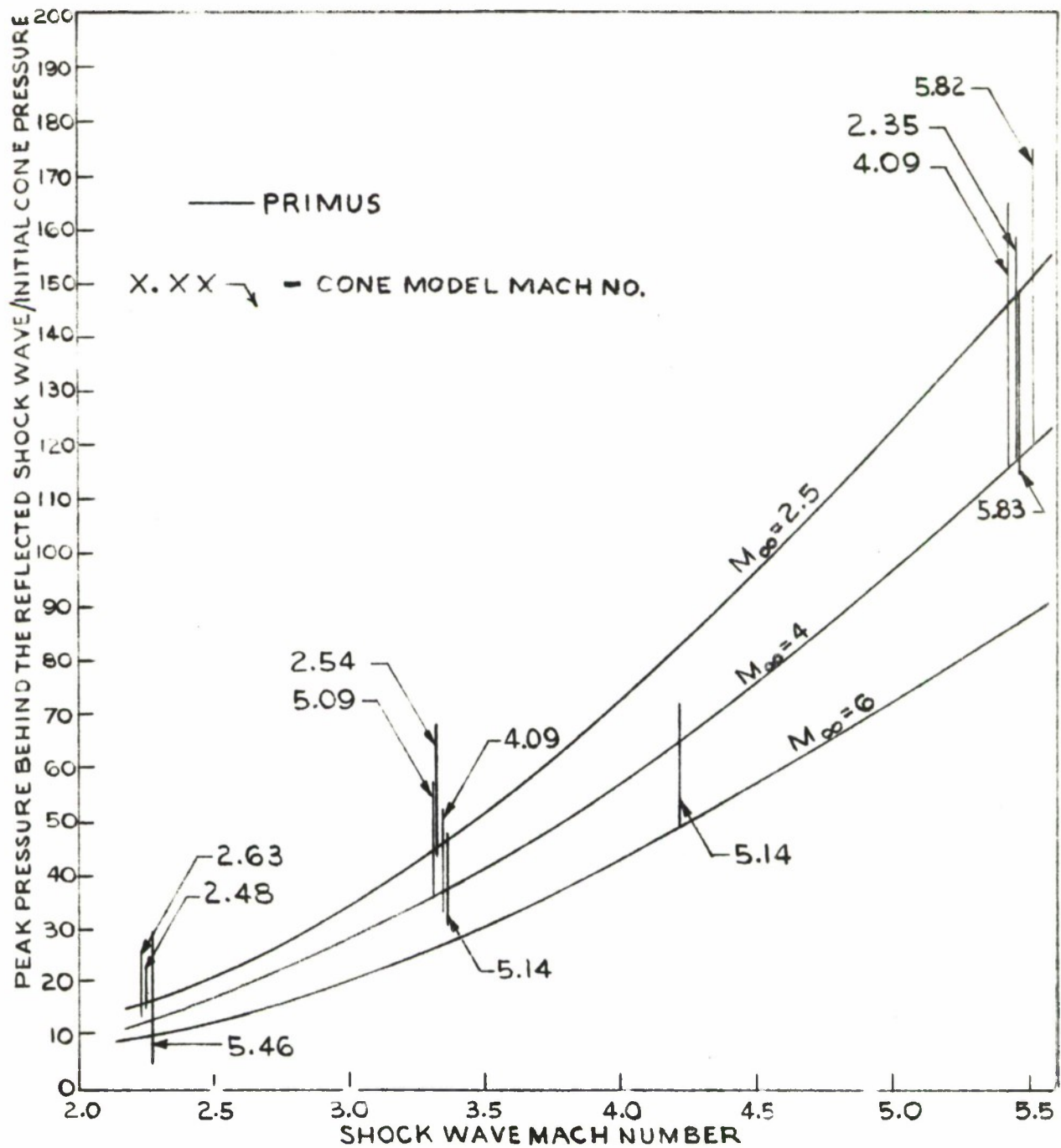


FIG. 8 RATIO OF THE PEAK PRESSURE BEHIND THE REFLECTED SHOCK WAVE TO THE INITIAL CONE PRESSURE VS. THE SHOCK WAVE MACH NUMBER - PRIMUS AND EXPERIMENT, 15° CONES

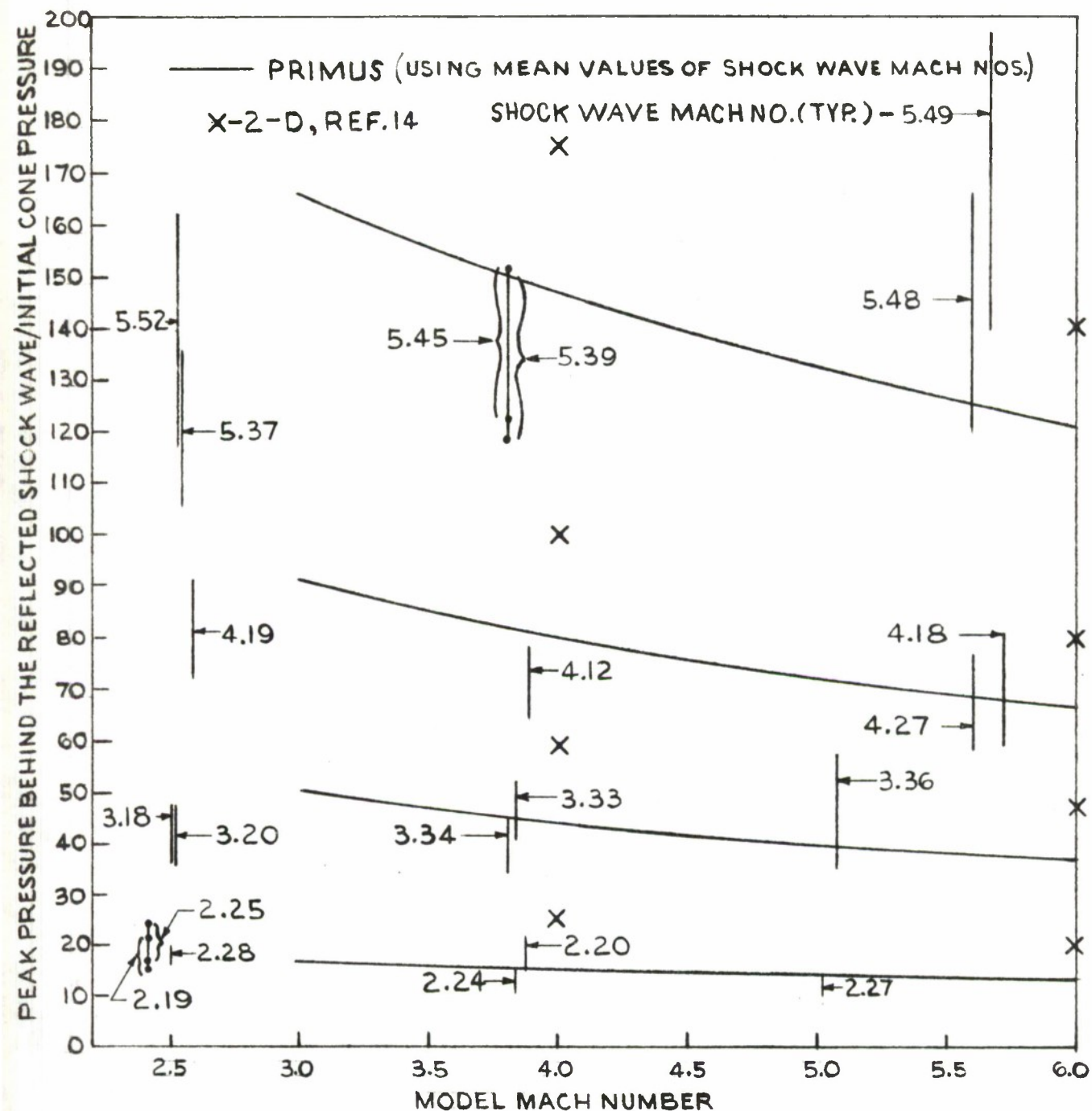


FIG. 9 RATIO OF THE PEAK PRESSURE BEHIND THE REFLECTED SHOCK WAVE TO THE INITIAL CONE PRESSURE VS. MODEL MACH NUMBER - PRIMUS, NOL, & EXPERIMENT, 9° CONE MODELS

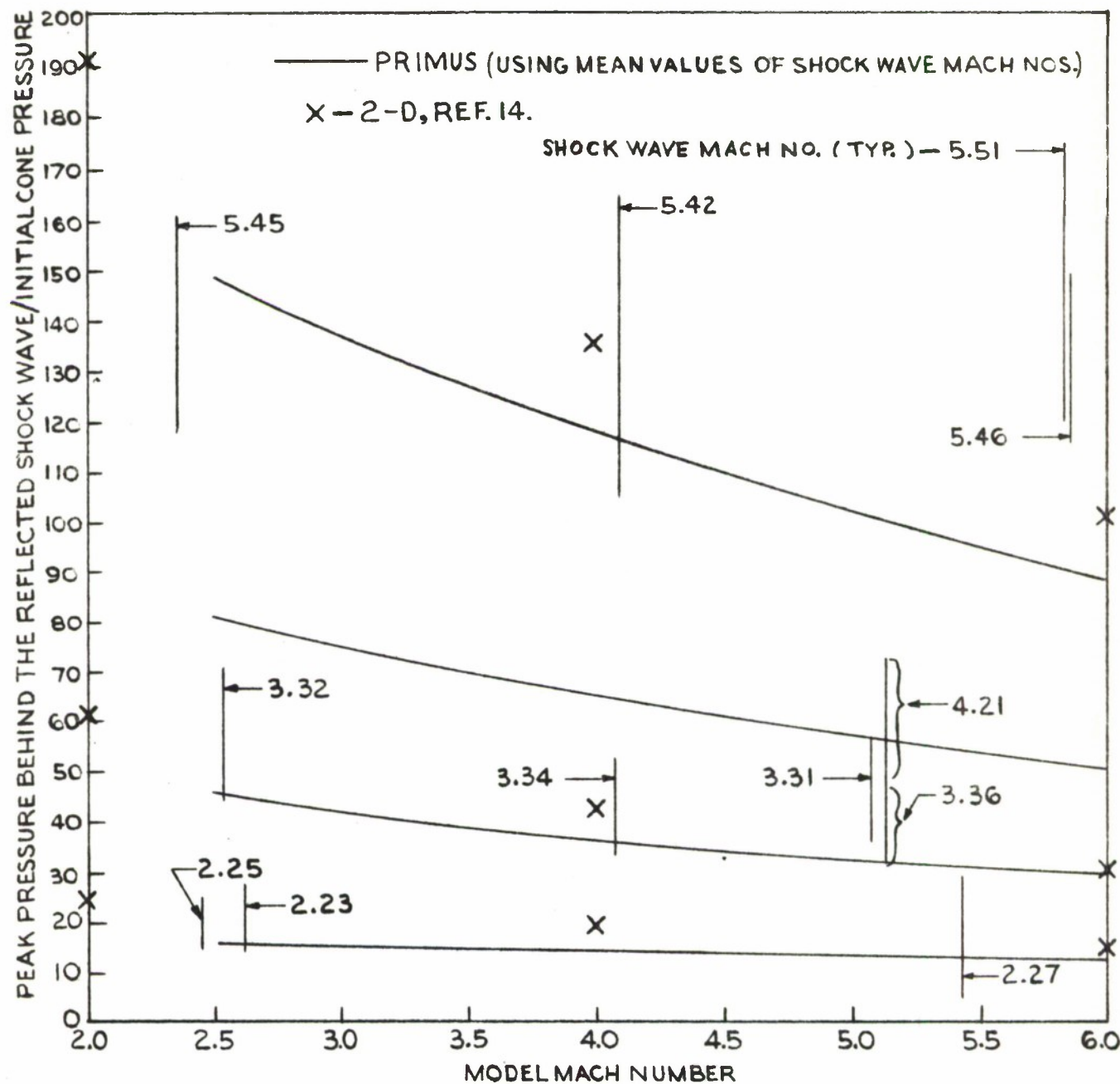


FIG.10. RATIO OF THE PEAK PRESSURE BEHIND THE REFLECTED SHOCK WAVE TO THE INITIAL CONE PRESSURE VS. MODEL MACH NUMBER- PRIMUS, NOL, & EXPERIMENT, 15° CONE MODELS

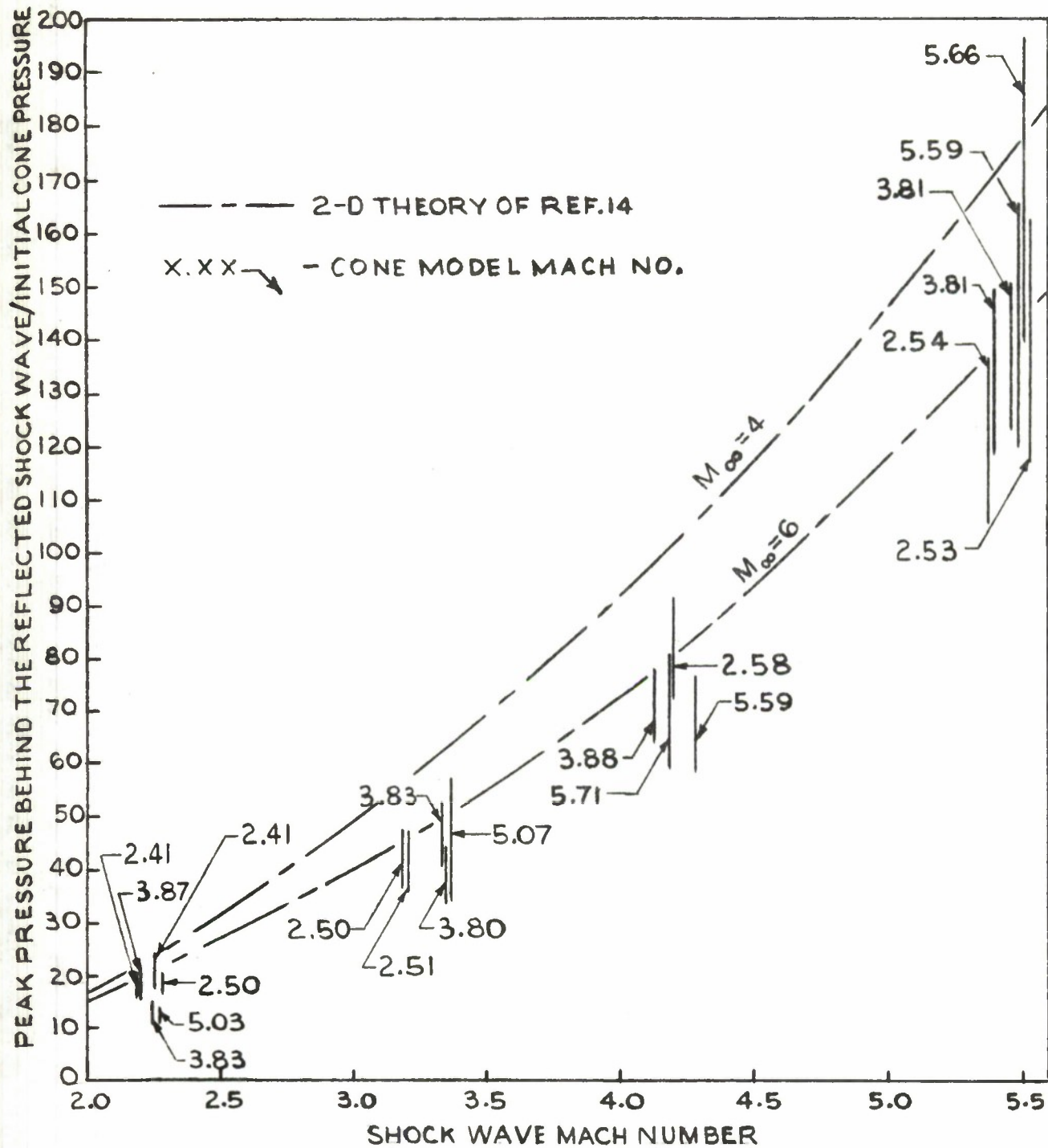


FIG.11 RATIO OF THE PEAK PRESSURE BEHIND THE REFLECTED SHOCK WAVE TO THE INITIAL CONE PRESSURE VS. THE SHOCK WAVE MACH NUMBER-THEORY AND EXPERIMENT, 9° CONE MODELS

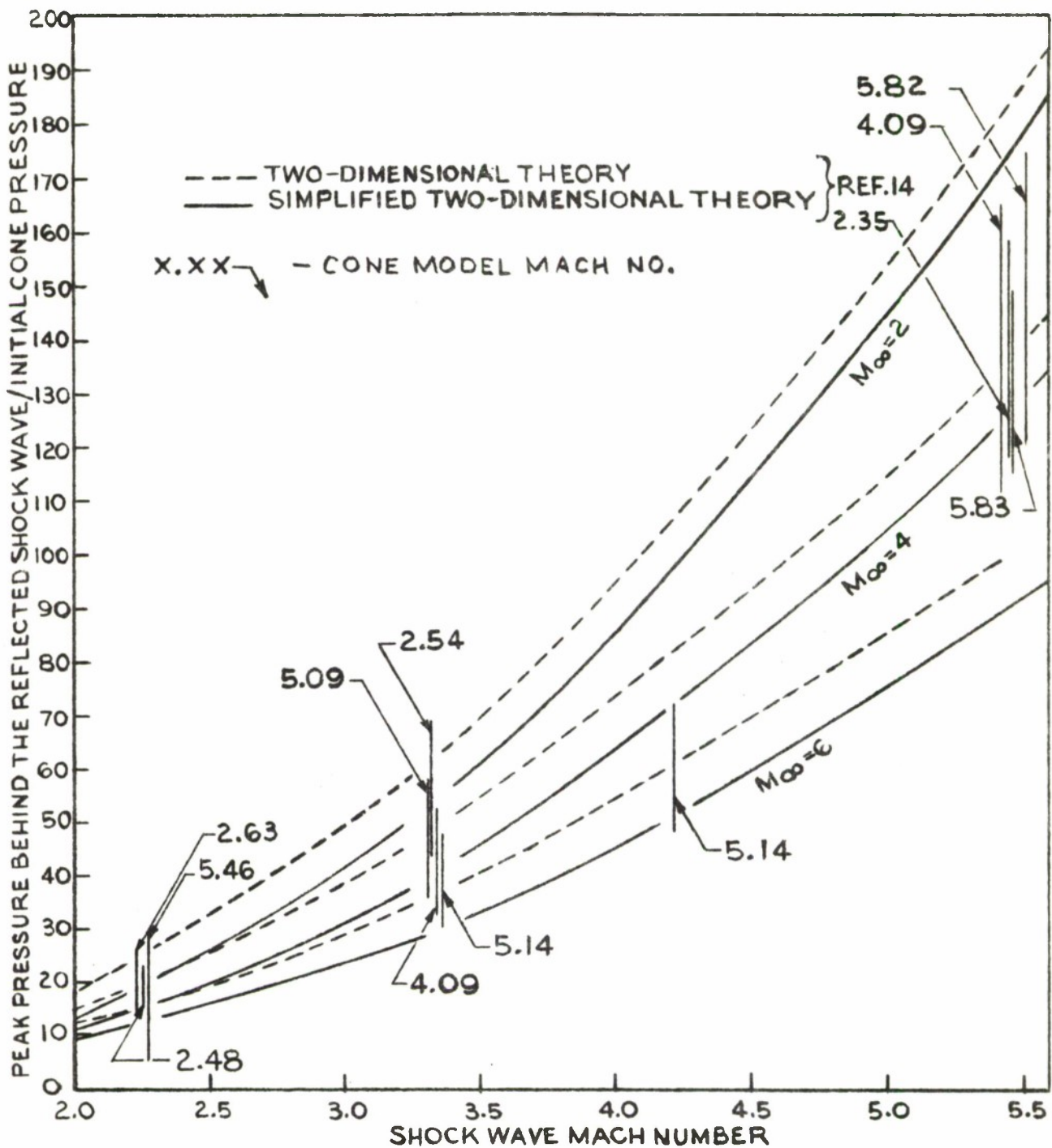
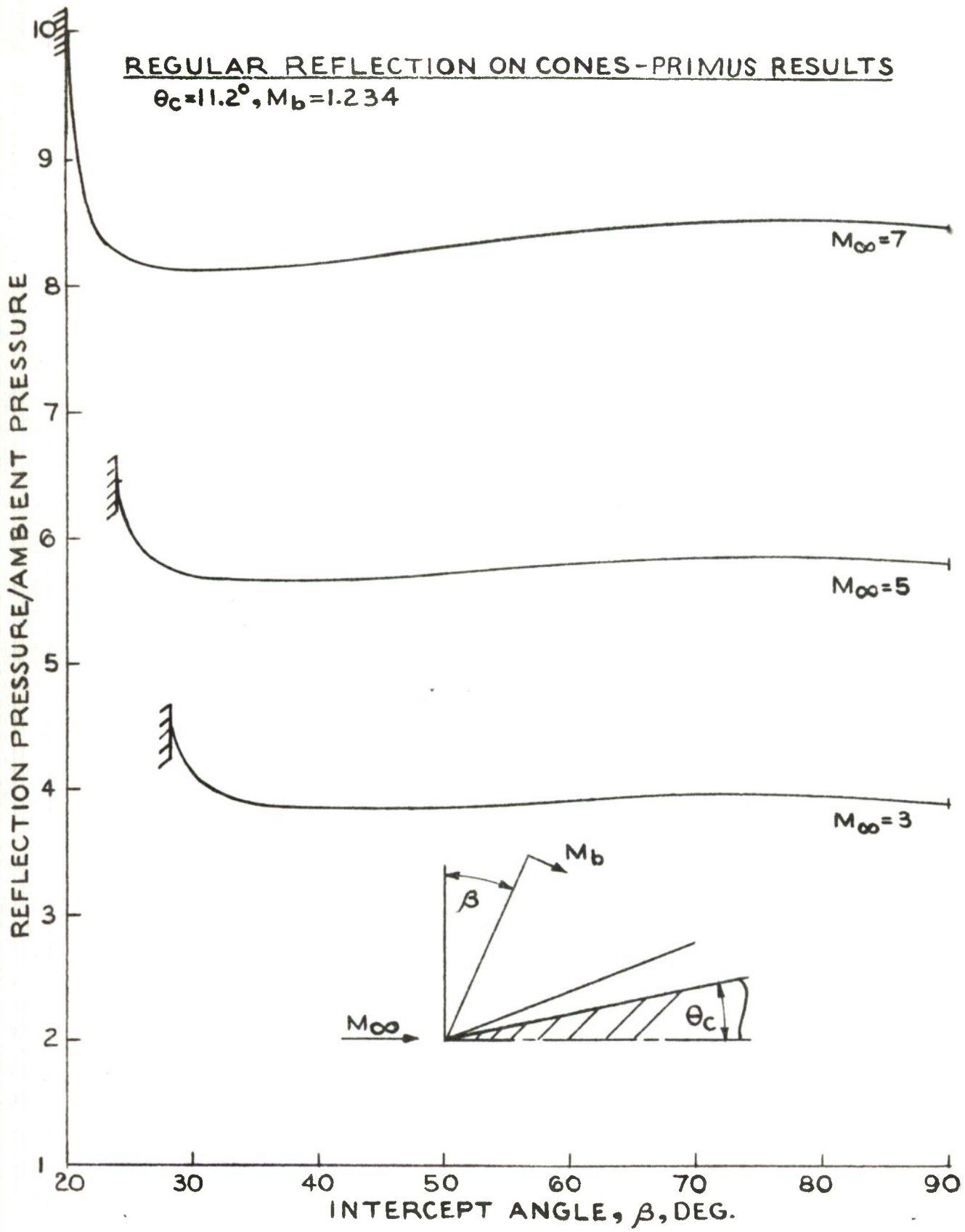
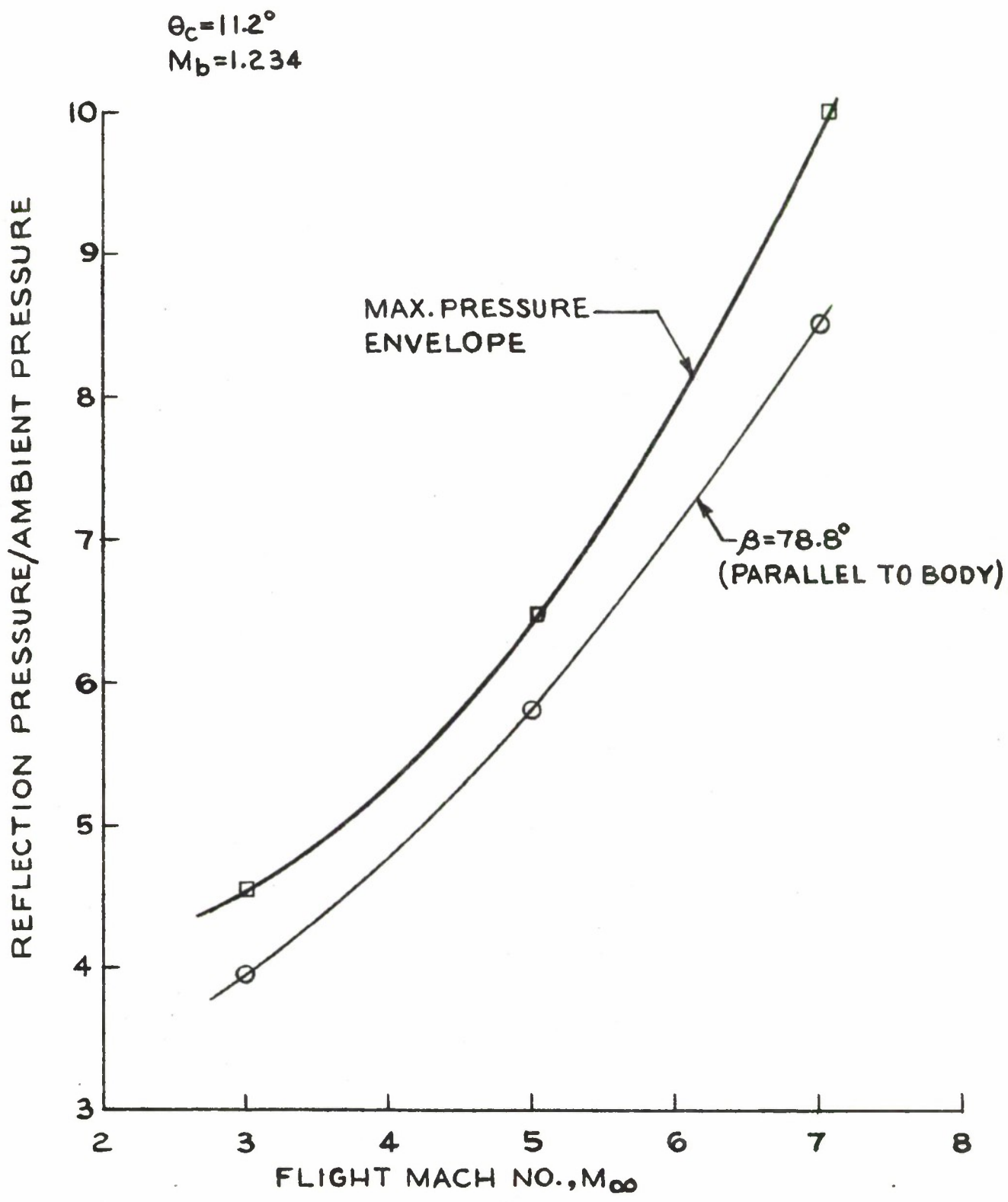


FIG.12 RATIO OF THE PEAK PRESSURE BEHIND THE REFLECTED SHOCK WAVE TO THE INITIAL CONE PRESSURE VS. THE SHOCK WAVE MACH NUMBER—THEORY AND EXPERIMENT, 15° CONE MODELS



COMPARISON OF MAXIMUM AND SIDE-ON PRESSURES
FOR REGULAR REFLECTION



COMPARISON OF TWO WEAK BLAST CASES FOR
VALIDITY OF HYPERSONIC SIMILITUDE

$$M_b = 1.234$$

$$K_N = M_\infty \sin \theta_c = 0.9712$$

— $M_\infty = 5, \theta_c = 11.2^\circ$
— $M_\infty = 10, \theta_c = 5.57^\circ$

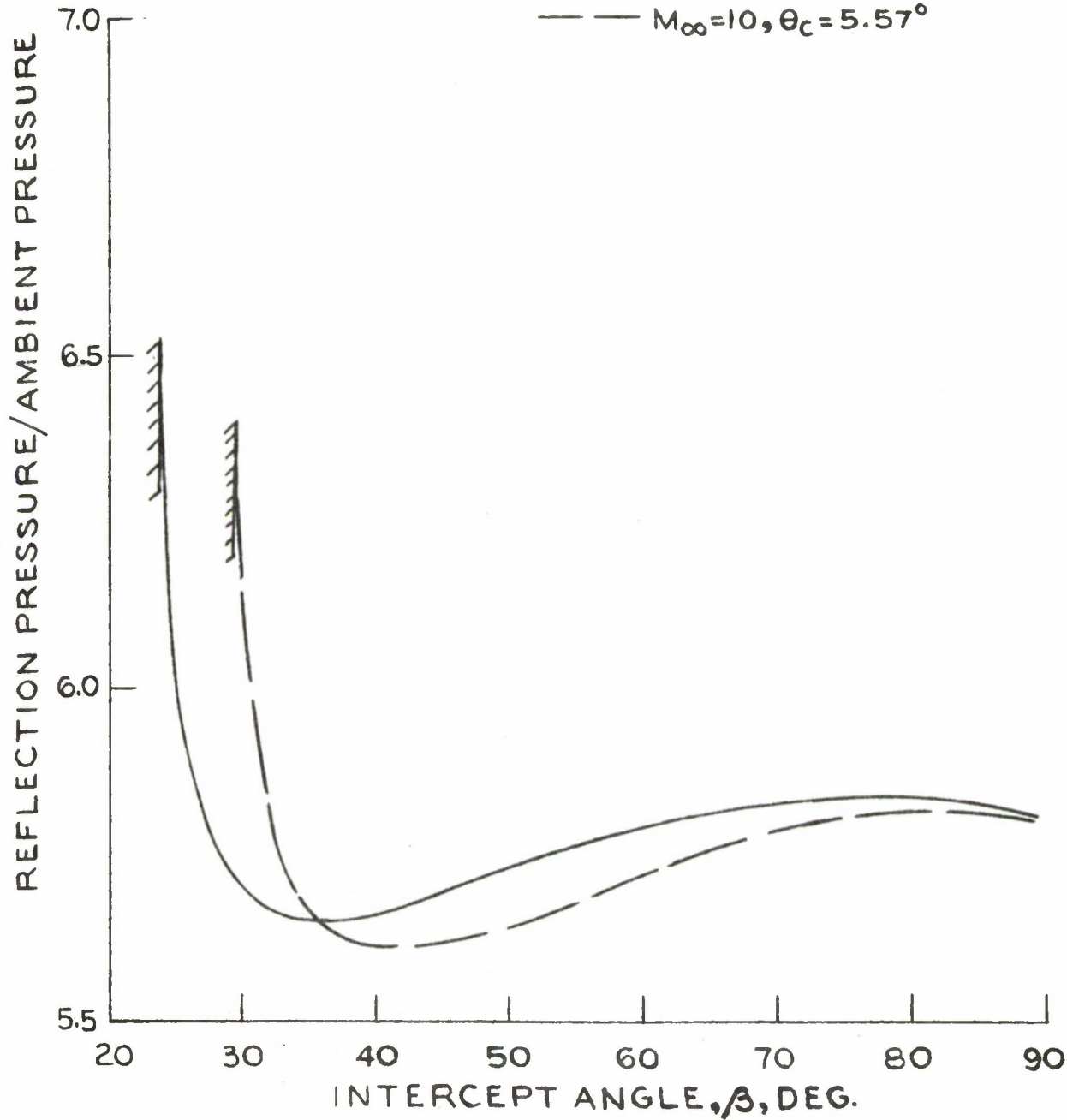


FIG.15.

DISTRIBUTION LIST

	<u>No. of</u> <u>Copies</u>
Commander Defense Documentation Center ATTN: TIPCR Cameron Station Alexandria, Virginia 22314	(2)
Director Advanced Research Projects Agency ATTN: Dr. J. Wade Washington, D. C. 20301	(1)
Director Weapons Systems Evaluation Group ATTN: CPT Donald E. McCoy, USN 400 Army-Navy Drive Washington, D. C. 20305	(1)
Director Institute of Defense Analysis 400 Army-Navy Drive Arlington, Virginia 22202	(1)
Director Defense Nuclear Agency ATTN: APSI (ARCHIVES) DDST APTL, Tech Lib (2) Washington, D. C. 20305	(4)
Headquarters Defense Nuclear Agency ATTN: SPAS (2) J. Moulton Ltc M. Kovel SPSS Washington, D. C. 20305	(3)

	<u>No. of</u> <u>Copies</u>
Commander, Field Command Defense Nuclear Agency ATTN: Tech Lib, FCWS-SC FCWD-C Kirtland AFB New Mexico 87115	(2)
Director Defense Intelligence Agency ATTN: DI-78 Washington, D. C. 20301	(1)
Commander US Army Materiel Command ATTN: AMCDL 5001 Eisenhower Avenue Alexandria, Virginia 22304	(1)
Commander US Army Materiel Command ATTN: AMCRD, MG S. C. Meyer 5001 Eisenhower Avenue Alexandria, Virginia 22304	(1)
Commander US Army Materiel Command ATTN: AMCRD, Dr. J.V.R. Kaufman 5001 Eisenhower Avenue Alexandria, Virginia 22304	(1)
Commander US Army Materiel Command ATTN: AMCRD-TE 5001 Eisenhower Avenue Alexandria, Virginia 22304	(1)
Commander US Army Materiel Command ATTN: AMCRD-TP 5001 Eisenhower Avenue Alexandria, Virginia 22304	(1)

	<u>No. of</u> <u>Copies</u>
Commander US Army Materiel Command ATTN: AMCRD-WN John F. Corrigan 5001 Eisenhower Avenue Alexandria, Virginia 22304	(1)
Director Ballistics Research Laboratories ATTN: J. Meszaros (2) G. Teel (1) R. Sedney (1) Aberdeen Proving Ground, Maryland 21005	(4)
Commander US Army Aviation Systems Command ATTN: AMSAV-E 12th & Spruce Streets St. Louis, Missouri 63166	(1)
Director US Army Air Mobility Research And Development Laboratory Ames Research Center Moffett Field, California 94035	(1)
Commander US Army Electronics Command ATTN: AMSEL-RD Fort Monmouth, New Jersey 07703	(1)
Commander US Army Missile Command ATTN: AMSMI-R AMCPM-MDE AMCPM-LCE AMCPM-PE Dr. Troy Smith Redstone Arsenal, Alabama 35809	(5)

	<u>No. of</u> <u>Copies</u>
Commander US Army Tank Automotive Command ATTN: AMSTA-RHFL Warren, Michigan 48090	(1)
Commander US Army Mobility Equipment Research & Development Center ATTN: TECH DOCU CEN, Cldg. 315 AMSME-RZT Fort Belvoir, Virginia 22060	(2)
Commander US Army Armaments Command ATTN: AMSAR-RD G. Chesnov Rock Island, Illinois 61201	(1)
PLASTEC US Army Picatinny Arsenal ATTN: SMUPA-FR-M-D Dover, New Jersey 07801	(1)
Commander US Army Picatinny Arsenal ATTN: A. J. Tenk D. Miller A. Loeb (3 cys) D. Waxler Dover, New Jersey	(6)
Commander US Army Weapons Command ATTN: AMSWE-RE AMSWE-RDF Rock Island, Illinois 61202	(2)

	<u>No. of</u> <u>Copies</u>
Commander US Army Safeguard Systems Command ATTN: SSC-DH, Mr. H. Solomonson, (3 cys) SSC-DRS, Mr. W. Hendry PO Box 1500 Huntsville, Alabama 35807	(4)
Commander US Army Safeguard Systems Command ATTN: SSC-SD, Dr. W. Mendes SSC, Mr. R. Freeman SSC-SD, Mr. H. Thames P.O. Box 1500 Huntsville, Alabama 35807	(3)
Safeguard System Manager Safeguard System Office ATTN: J. J. Shea 1300 Wilson Boulevard Arlington, Virginia 22209	(1)
Director US Army Advanced Materiel Concept Agency 2461 Eisenhower Avenue Alexandria, Virginia 22314	(1)
Commander US Army Harry Diamond Labs. ATTN: AMXDO-TD/002 AMXDO-NP, F. M. Wimenitz Washington, D. C. 20438	(2)
Commander US Army Materials and Mechanics Research Center ATTN: Mr. J. Dignam Watertown, Massachusetts 02172	(1)

	<u>No. of</u> <u>Copies</u>
Commander US Army Combat Developments Command Air Defense Agency Fort Bliss, Texas 79916	(1)
Commander US Army Combat Developments Command Nuclear Agency ATTN: CDINS-E, Maj. E. Starbird Fort Bliss, Texas 79916	(1)
Commander US Army Air Defense Command ATTN: ADGES ENT Air Force Base Colorado 80912	(1)
HQDA (DARD-MSN, MAJ D. Griggs) Washington, D. C. 20310	(1)
Director Advanced Ballistic Missile Defense Agency Commonwealth Building ATTN: CRDABM-NE, Ltc E. V. DeBoeser 1320 Wilson Boulevard Arlington, Virginia 22209	(1)
Director Advanced Ballistic Missile Defense Agency ATTN: Marcus Whitfield W. Loomis P.O. Box 1500 Huntsville, Alabama 35807	(2)

	<u>No. of</u> <u>Copies</u>
Site Defense Project Office USA SAFSCOM P.O. Box 1500 ATTN: C. D. Richardson H. Thames Huntsville, Alabama 35807	(2)
Headquarters US Atomic Energy Commission ATTN: Div. of Mil. Appl. Washington, D. C. 20545	(1)
Headquarters US Naval Materiel Command ATTN: 03L Washington, D. C. 20360	(1)
Chief of Naval Operation ATTN: OP-75 Department of the Navy Washington, D. C. 20350	(1)
Commander US Naval Weapons Center China Lake, California 93555	(1)
Commander US Naval Weapons Evaluation Fac. Kirtland AFB, Albuquerque New Mexico 87117	(1)
Commander US Naval Ordnance Lab ATTN: Code 121, Navy Nuclear Programs Office Code 241, Joseph Petes Code 312, Mr. S. Hastings Silver Spring, Maryland 20910	(3)
HQ USAF (AFRST) Washington, D. C. 20330	(1)

	<u>No. of</u> <u>Copies</u>
AFSC (XR;SD/DE) Andrews AFB Washington, D. C. 20331	(2)
AFWL/AFSC (DDGL, Tech Lib; DEV, Dr. H. Cooper; Mr. A. Sharp Kirtland AFB New Mexico 87117	(3)
AFFDL (Mr. E. Pugh) Wright-Patterson AFB Ohio 45433	(1)
Director Lawrence Livermore Laboratory P.O. Box 808 Livermore, California 94550	(1)
NASA Ames Research Laboratory ATTN: Mr. R. Cutler Moffett Field, California 94035	(1)
USA SAFSCOM P.O. Box 1500 ATTN: SSC-TEM, Mr. N. Hurst Huntsville, Alabama 35807	(1)
Los Alamos Scientific Laboratory ATTN: Docu Control for Dr. T. Talley P.O. Box 1663 Los Alamos, New Mexico 87544	(1)
Sandia Laboratories ATTN: R. Pope B. Caskey P.O. Box 5800 Albuquerque, New Mexico 87115	(1)

	<u>No. of Copies</u>
Aerospace Corporation ATTN: Dr. Taylor Dr. A. Field 2350 E. El Segundo Blvd El Segundo, California 90245	(2)
Bell Telephone Laboratories ATTN: F. Prendergast Mead F. Stevens Whippany Rd. Whippany, New Jersey 07981	(2)
General Electric Company Tempo Center for Advanced Studies ATTN: Mr. W. Chan 816 State Street P.O. Drawer QQ Santa Barbara, California 93102	(1)
Kaman AviDyne Division of Kaman Sciences Corp. 83 Second Avenue ATTN: E. S. Criscione N. P. Hobbs R. Reutnik Northwest Industrial Park Burlington, Massachusetts 01803	(3)
Kaman Sciences Corporation ATTN: R. Keefe D. Sachs 1700 Garden of the Gods Road Colorado Springs, Colorado 80907	(2)
Martin Marietta Corporation Orlando Division ATTN: H. Rosenthal G. Foteio G. Aiello P.O. Box 5837 Orlando, Florida 32805	(3)

	<u>No. of</u> <u>Copies</u>
McDonnell-Douglas Company ATTN: C. P. Gardiner Site Defense Office 5301 Bolsa Avenue Huntington Beach, California 92647	(2)
Stanford Research Institute ATTN: W. B. Reuland 306 Wynn Drive, NW Huntsville, Alabama 35805	(1)
Stanford Research Institute ATTN: Dr. H. E. Lindberg 333 Ravenswood Avenue Menlo Park, California 94025	(1)
SETAC Division Teledyne Brown Engineering 300 Sparkman Drive Huntsville, Alabama 35805 ATTN: R. C. Kolyer R. E. Patrick	(2)
Aeronautical Research Associates of Princeton, Inc. (ARAP) 50 Washington Road Princeton, New Jersey 08548	(1)
<u>Aberdeen Proving Ground</u> Ch, Tech Lib Marine Corps Ln Ofc CDC Ln Ofc Dir, USAMSA ATTN: Dr. J. Sperazza	(4)

Unclassified

Security Classification

DOCUMENT CONTROL DATA - R & D

(Security classification of title, body of abstract and indexing annotation must be entered when the overall report is classified)

1. ORIGINATING ACTIVITY (Corporate author) Engineering Sciences Division Feltman Research Laboratory Picatinny Arsenal		2a. REPORT SECURITY CLASSIFICATION Unclassified
2b. GROUP		
3. REPORT TITLE Shock-Shock Interaction Studies for Weak Incident Shocks		
4. DESCRIPTIVE NOTES (Type of report and inclusive dates) Technical Report		
5. AUTHOR(S) (First name, middle initial, last name) Henry E. Hudgins Eugene M. Friedman		
6. REPORT DATE December 1973	7a. TOTAL NO. OF PAGES 86	7b. NO. OF REFS 25
8a. CONTRACT OR GRANT NO.	9a. ORIGINATOR'S REPORT NUMBER(S) PATR 4590	
b. PROJECT NO.	9b. OTHER REPORT NO(S) (Any other numbers that may be assigned this report)	
c. AMCMS Code 5911.21.20676	d.	
10. DISTRIBUTION STATEMENT Approved for public release; distribution unlimited		
11. SUPPLEMENTARY NOTES	12. SPONSORING MILITARY ACTIVITY Defense Nuclear Agency Washington, DC 20305	

13. ABSTRACT

The shock-shock interaction problem for weak incident waves impinging on a supersonic cone has been examined. The purpose of this study was to establish methods for predicting surface pressures since existing methods have been found inadequate for practical problems with weak blast waves. It is shown in this study that one-dimensional theory, which works well for strong blast waves, fails when the components normal to the surface of the flight velocity and of the blast particle velocity become comparable. As a consequence, an axisymmetric two-dimensional solution method was developed using a "primary wave" approximation. This approach has been automated in the PRIMUS computer code. The predictions from the code have been checked against experiment and other theory. The comparisons are presented and the agreement is quite good. The code was also used to predict the cone pressures for DNA Sled Test experiments. The results are presented and compared with the experimental results and other theoretical predictions.

This study established that for weak blast waves the maximum pressure for regular reflection occurs at the Mach reflection limit, not at side-on intercept. The question of whether reflection pressures are even higher on the Mach reflection side of the boundary was examined, but existing

DD FORM 1 NOV 1973

REPLACES DD FORM 1473, 1 JAN 64, WHICH IS
OBSOLETE FOR ARMY USE.

Unclassified
Security Classification

Unclassified

Security Classification

14. KEY WORDS	LINK A		LINK B		LINK C	
	ROLE	WT	ROLE	WT	ROLE	WT
Shock - shock interaction Weak Waves Regular reflection Finite - difference methods Primary wave methods One - dimensional unsteady flow Two - dimensional unsteady flow Conical flow Wedge flow						

Shock Wave
Blast Wave
Weak Front Wave

Unclassified
Security Classification